Faculty of Engineering Porto University
Master Dissertation

Distribution network of ice water optimization

Author
Eva Lopes Gomes

Supervisors
Prof. Abel Ilah Rouboa (FEUP)
Eng. Vitor Emanuel Duarte Santos

U.PORTO
FEUP FACULDADE DE ENGENHARIA UNIVERSIDADE DO PORTO

Master in Mechanical Engineering

September 2025

Abstract

This dissertation focuses on the study and evaluation of the ice water network in an industrial facility, highlighting key issues related to thermal gains along the distribution lines, hydraulic pressure losses, and their impact on the overall efficiency of the refrigeration system. The motivation for this work arises from the growing need for more energy-efficient solutions that reduce operational costs while maintaining the reliability of cooling for production processes.

The work begins with a literature review that contextualizes the evolution of refrigeration systems, presenting proven industrial solutions and innovative alternatives under development. The existing ice water network is then described, including the thermal cycle, the frozen water system, and the distribution layout. A detailed thermal and hydraulic analysis is performed on a machine-by-machine and line-by-line basis, quantifying hourly heat loads, heat transfer, and pressure drops. Based on these results, key performance indicators (KPIs) are defined, focusing on heat gain, pressure drop, and overall system efficiency. Improvement proposals are associated with each KPI, with a balanced discussion of their advantages and limitations.

In addition to general optimization measures, the study emphasizes the potential of implementing more effective solution strategies, such as separating consumers based on their cooling temperature requirements.

The study concludes that the network provides significant potential for optimization, particularly in improving pipe insulation and lowering pressure drops in specific sections. Defining KPIs proved crucial for measuring performance and guiding improvements. Future work should focus on gathering additional data, testing proposed measures, and implementing advanced monitoring technologies to further increase efficiency and sustainability.

Resumo

Esta dissertação tem como foco o estudo e a avaliação da rede de água gelada em uma instalação industrial, identificando os principais problemas relacionados aos ganhos térmicos ao longo das linhas de distribuição, às perdas de carga hidráulica e ao impacto desses fatores na eficiência global do sistema de refrigeração. A motivação para este trabalho decorre da crescente demanda por soluções energeticamente mais eficientes, capazes de reduzir os custos operacionais e, ao mesmo tempo, assegurar a confiabilidade do fornecimento de resfriamento aos processos produtivos.

O trabalho desenvolvido inicia-se com uma revisão bibliográfica que contextualiza a evolução dos sistemas de refrigeração, apresentando tanto soluções industriais consolidadas quanto alternativas inovadoras em desenvolvimento. Em seguida, é descrita a rede de água gelada existente, incluindo o ciclo térmico, o sistema de água congelada e o arranjo de distribuição. Foi realizada uma análise térmica e hidráulica detalhada, máquina a máquina e linha a linha, quantificando cargas térmicas horárias, transferências de calor e perdas de pressão. Com base nesses resultados, foram definidos indicadores-chave de desempenho (KPIs), com ênfase nos ganhos térmicos, perdas de carga e eficiência global do sistema. A cada KPI foram associadas propostas de melhoria, acompanhadas de uma discussão equilibrada sobre suas vantagens e limitações.

Além das medidas gerais de otimização, o estudo ressalta a importância de estratégias mais eficientes, como a separação dos consumidores de acordo com suas necessidades de temperatura.

Conclui-se que a rede apresenta um potencial significativo de otimização, em especial por meio da melhoria do isolamento térmico das tubulações e da redução de perdas de carga em trechos específicos. A definição de KPIs mostrou-se essencial para a quantificação do desempenho e para a orientação das ações de melhoria. Trabalhos futuros devem priorizar a ampliação da base de dados, a testagem das medidas propostas e a integração de tecnologias avançadas de monitoramento, de forma a potencializar ainda mais a eficiência e a sustentabilidade do sistema.

Acknowledgements

This work was completed through the collaboration, encouragement, and dedication of many people. I extend my sincere gratitude to all who contributed to making this project a reality.

I am especially grateful to Professor Abel Ilah Rouboa, my Master's supervisor in Mechanical Engineering, for his guidance, support, and readiness to help throughout my project. I also thank my company supervisor at BEL, Vitor Santos, for his support, patience, and valuable assistance, which were essential to the completion of this project.

Contents

1 Introduction **1**

1.1 Framing and motivation . . . 1

1.2 Objectives . . . 1

1.3 Methodology . . . 2

1.4 Structure . . . 2

1.5 Company . . . 3

2 Literature Review **7**

2.1 Current status . . . 7

2.2 Latest developments . . . 8

2.3 Premise of project . . . 8

3 Ice Water Network **11**

3.1 Ice Water Thermal Cycle . . . 11

3.1.1 Ice Water Tank . . . 12

3.1.2 Compressors CP1 and CP2 . . . 13

3.2 Components of ice water line . . . 13

3.2.1 Pumps of ice water . . . 13

3.2.2 Properties of the Piping . . . 14

3.2.3 Most Common Valve Types and Typical Applications . . . 14

3.3 Network Layout . . . 19

3.3.1 Network A . . . 19

3.3.2 Network B . . . 21

4 Hydraulic and Heat Studies of the Site **25**

4.1 Hydraulic study . . . 25

4.1.1 Local Pressure Losses Analysis . . . 26

4.1.2 Cavitation Verification . . . 29

4.2 Heat Transmission Study . . . 30

4.2.1 Initial Conditions and Parameters . . . 30

4.2.2 Thermal Resistance and Heat Transfer to Ambient . . . 30

4.2.3 Convective Heat Transfer Coefficients . . . 32

5 Identification of KPIs and OPIs **33**
5.1 Main OPIs 33
5.2 Main KPIs 36
5.2.1 COP 36
5.2.2 SEC 38
5.2.3 Central refrigeration plant Availability 39

6 Discussion of Results **41**
6.1 Impact of Inlet Temperature on System Performance 41
6.1.1 Heat Gain in Distribution Lines vs. Production Loads 42
6.1.2 Opportunities for Network Redesign 42
6.1.3 Opportunities for Cooling Central Redesign 42
6.1.4 Serum Cooling Capacity 43
6.2 Summary of Findings 43

7 Conclusions and Future Work **45**
7.1 Conclusion 45
7.1.1 Thermal performance assessment 45
7.1.2 Hydraulic study 45
7.1.3 Key and Operational Performance Indicators 46
7.1.4 Main conclusions 46
7.2 Future Works 47

A Appendix **51**
A.1 Diagram of circuit of chill compressors 51
A.2 Catalogs of pumps 52
A.2.1 Line A 52
A.2.2 Line B 53
A.3 Physical properties of air and water 56
A.3.1 Water properties 56
A.3.2 Air properties 57
A.4 Data for each section of the lines 58
A.5 Pressure drop in different sections of each line 61
A.6 Heat gain in different sections of each line 65
A.7 Frigorific capacity and inlet and return temperatures by the hour 68

Nomenclature

Acronyms

PID Process Diagram

KPI Key Performance Indicator

OPI Operational Performance Indicator

NPSH Net Positive Suction Head Available

COP Coefficient of performance

MTBF Mean Time Between Failure

MTTR Mean Time To Repair

SEC Specific Energy Consumption

TR Tons of Refrigeration

Greek Symbols

Δ Variation

$\boldsymbol{\mu}$ Dynamic viscosity (Pa.s)

$\boldsymbol{\nu}$ Kinematic viscosity (m^2/s)

$\boldsymbol{\rho}$ Density (kg/m^3)

$\boldsymbol{\beta}$ Viscosity ratio

$\boldsymbol{\epsilon}$ Roughness (mm)

Latin Symbols

$\boldsymbol{c_p}$ Specific heat capacity (kJ/kg.K)

$\boldsymbol{D}$ Diameter of the pipe (mm)

$\boldsymbol{f}$ Darcy friction factor

$\boldsymbol{g}$ Gravitational acceleration (m/s^2)

$\boldsymbol{Gr}$	Grashof number
$\boldsymbol{H}$	Head (m)
$\boldsymbol{h}$	Heat transfer coefficient (W/m.k^2)
$\boldsymbol{h_l}$	Local head loss (mH2O)
$\boldsymbol{k_l}$	Local loss coefficient
$\boldsymbol{k}$	Thermal conductivity
$\boldsymbol{Q}$	Heat (W)
$\boldsymbol{l}$	Pipe length (m)
$\boldsymbol{L_c}$	Characteristic Length (m)
$\boldsymbol{m}$	Mass (kg)
$\boldsymbol{\dot{m}}$	Mass flow rate (kg/s)
$\boldsymbol{Nu}$	Nusselt number
$\boldsymbol{p}$	Pressure (Pa)
$\boldsymbol{Pr}$	Prandtl number
$\boldsymbol{W}$	Electrical energy consumed (W)
$\boldsymbol{r}$	Radius (mm)
$\boldsymbol{Re}$	Reynolds number
$\boldsymbol{Ra}$	Rayleigh number
$\boldsymbol{t}$	Time (s)
$\boldsymbol{T}$	Temperature (^{o}C)
$\boldsymbol{v}$	Mean fluid velocity (m/s)
$\boldsymbol{V}$	Volume (m^3)
$\boldsymbol{\dot{V}}$	Volumetric flow rate (m^3/s)
$\boldsymbol{z}$	Height (m)

List of Figures

1.1 Flowchart of BEL Portugal's production process 4

3.1 Schematic of the ammonia circuit (see Figure A.1 for a more detailed version). 11
3.2 Vapor-compression cycle represented in T–s and P–h diagrams. 12
3.3 Diagram of the different layers of the pipe 14
3.4 Two-Port Globe Valve (Manual actuation) 15
3.5 Three-Port Globe Valve (Manual actuation) 15
3.6 Symbols of globe valves, manual and piston, respectively 16
3.7 Control Valve (Manual actuation) 16
3.8 Control Valve (Diaphragm Actuation) 17
3.9 Symbols of control valves, manual and diaphragm, respectively 17
3.10 Butterfly Valve (Manual Actuation) 17
3.11 Symbols of butterfly valves, manual and piston, respectively 18
3.12 Angle Valve (Piston Actuation) 18
3.13 Symbols of 3 way control and angular valves, respectively 19
3.14 Layout of Line A (part 1) 20
3.15 Layout of Line A (part 2) 20
3.16 Layout of Line A (part 3) 21
3.17 Layout of Line B (part 1) 22
3.18 Layout of Line B (part 2) 22
3.19 Layout of Line B (part 3) 23
3.20 Layout of Line B (part 4) 23

4.1 Heat Loss in an Insulated Pipe 31

5.1 Temperature of inlet water in a day 33
5.2 Temperature of inlet water in a week 34
5.3 Temperature of outlet water in a day 35
5.4 Temperature of outlet water in a week 36
5.5 Frigorific Capacity Requirements in a day 37

A.1 Diagram of circuit of chill compressors 51
A.2 Manometric height in function of delivery and bomb type in catalog EFAFLU 52
A.3 Height graphic in catalog EFAFLU 53

A.4 Manometric height in function of delivery and bomb type in catalog LOWARA 53
A.5 Height graphic in catalog LOWARA 54
A.6 NPSH, power and manometric height of pump in catalog LOWARA 55
A.7 Physical properties of water at different temperatures 56
A.8 Physical properties of air at different temperatures 57
A.9 Data and properties of each section in the line A1 58
A.10 Data and properties of each section in the line A2 58
A.11 Data and properties of each section in the line B1 59
A.12 Data and properties of each section in the line B2 60

List of Tables

4.1 Local Loss coefficients of Different Elements 26
4.2 Head Losses by Section A1 27
4.3 Head Losses by Section A2 27
4.4 Head Losses by Section B1 28
4.5 Head Losses by Section B2 29
4.6 Calculated thermal parameters for Lines A and B 32

5.1 Failures, MTBF, Revisions, MTTR and Availability per month 39

A.1 Table of Pressure Drop in different sections of Line A1 61
A.2 Table of Pressure Drop in different sections of A2 62
A.3 Table of Pressure Drop in different sections of B1 63
A.4 Table of Pressure Drop in different sections of B2 64
A.5 Table of Q gain in different sections of A1 65
A.6 Table of Q gain in different sections of A2 65
A.7 Table of Q gain in different sections of B1 66
A.8 Table of Q gain in different sections of B2 67
A.9 Schedule Water Temperature and refrigeration capacity necessary Data 68

Chapter 1

Introduction

This work is carried out by Eva Lopes Gomes, in the second semester of the academic year 2024/2025, with Professor Abel Rouboa as advisor, within the scope of the dissertation for the master's degree in mechanical engineering, with a view to optimizing an ice water distribution network.

1.1 Framing and motivation

The present dissertation is developed within the scope of mechanical engineering and industrial utilities management. The project was carried out at BEL (Bel Portugal, S.A.), a leading food industry company specializing in dairy products and cheese manufacturing, within its Maintenance Department. This department is responsible for the operation, monitoring, and continuous improvement of essential energy and utility systems that support production, including ice water networks.

The project's main objective is twofold:

1. To provide complete documentation of the chilled water distribution network layout, ensuring that every branch, valve, heat exchanger, and connection is clearly identified and represented in updated technical drawings.

2. To define and validate KPIs for continuous monitoring of the utility's efficiency, enabling data-driven decisions for energy optimization and operational reliability.

The ice water line network was built several years ago. It has since been expanded and modified many times, often without full integration into a centralized documentation system. Therefore, a comprehensive study of its current configuration is necessary. This involves mapping the current system, evaluating its operational performance, and identifying areas for hydraulic balancing, insulation improvements, or component modernization to enhance efficiency and lower operating costs.

For mechanical engineers, the ability to integrate thermofluid analysis and energy management into chilled water systems represents a direct contribution to both environmental goals and economic performance.

1.2 Objectives

The objectives of this work are outlined to achieve an in-depth understanding and provide innovative solutions to the challenges presented in the study. Therefore, the specific objectives of this project are as follows:

- Full documentation of the ice water distribution network layout
- Study and alignment with the good practices group
- Alignment with external partner company
- Identification of KPIs for monitoring the utility's efficiency

1.3 Methodology

The methodology proposed for this project encompasses a series of detailed and interconnected steps. The following activities will be carried out systematically to ensure the efficiency and effectiveness of the project:

- Preparation of PID process diagram of the current network: Organize already existing information with on-site measurement of all components that could contribute to pressure losses in the system in a single, comprehensive drawing representing ice water lines.
- Hydraulic study for process optimization: Estimate the pressure losses along the ice water network and propose improvement solutions.
- Study of heat transmission to improve the plant's energy efficiency: Estimate the heat gains along the ice water network and cooling necessities, and propose improvement solutions.
- Preparation of project dossier

1.4 Structure

This dissertation is structured as follows:

1. Literature Review (State of the art):

   In this section, a brief historical contextualization is presented to provide a light introduction to the topic, as well as existing solutions and alternatives with implementation in the market and demonstrated reliability, the latest alternatives and solutions developed, even in a prototype or concept phase, the various motivations, for carrying out the work and commercial justifications. All the constraints to the project and the first difficulties felt, as well as the ideas that were the basis of the first approaches to the project.

2. Ice water Network:

   In this chapter, the background of the thermal process is detailed, including the existing methodology of the cooling system cycle. Then, the Frozen water system components and how they work, as well as the network layout.

3. Hydraulic and Heat studies of the site:

   This chapter presents a thermal performance study of each machine operating on the site, evaluated on an hourly basis throughout a representative operating cycle. For each machine, the analysis quantifies the heat load generated or absorbed during operation. And finally, the steps and calculations taken in the hydraulic and heat transmission studies of each line are detailed. The results of this machine-by-machine heat load assessment are then compared with the heat transmission studies of the lines.

4. Identification of possible KPI:

   This chapter begins by clearly defining what a KPI and OPI are and explaining their role. Following the definition, the chapter details the methodology used to identify relevant KPIs and OPIs for the system under study. For each KPI, proposed improvement solutions are presented.

5. Discussion:

   The Discussion chapter interprets and analyzes the results obtained throughout the study and the objectives established at the outset. The chapter also evaluates the practical implications of the results, identifying strengths, weaknesses, and potential areas for improvement.

6. Conclusion and Future Works:

   This chapter summarizes the key findings of the study, highlighting how the objectives were met, the main results achieved, and any limitations or constraints that may have influenced the outcomes. The chapter then outlines recommended future actions, such as further data collection, refinement of methods, testing of proposed improvements, or adoption of advanced technologies.

1.5 Company

BEL Portugal, S.A., part of the Bel Group, is a leading company in the dairy industry, specializing in the production of processed cheese, fresh cheese, and other dairy-based products. The Bel Group, headquartered in France, operates in over 40 countries, with brands such as The Laughing Cow, Babybel, and Boursin, recognized worldwide.

The BEL Portugal's production facility, where the project was carried out, is located in Vale de Cambra, where it combines advanced manufacturing technologies with strict quality control processes to ensure compliance with both national and international food safety regulations.

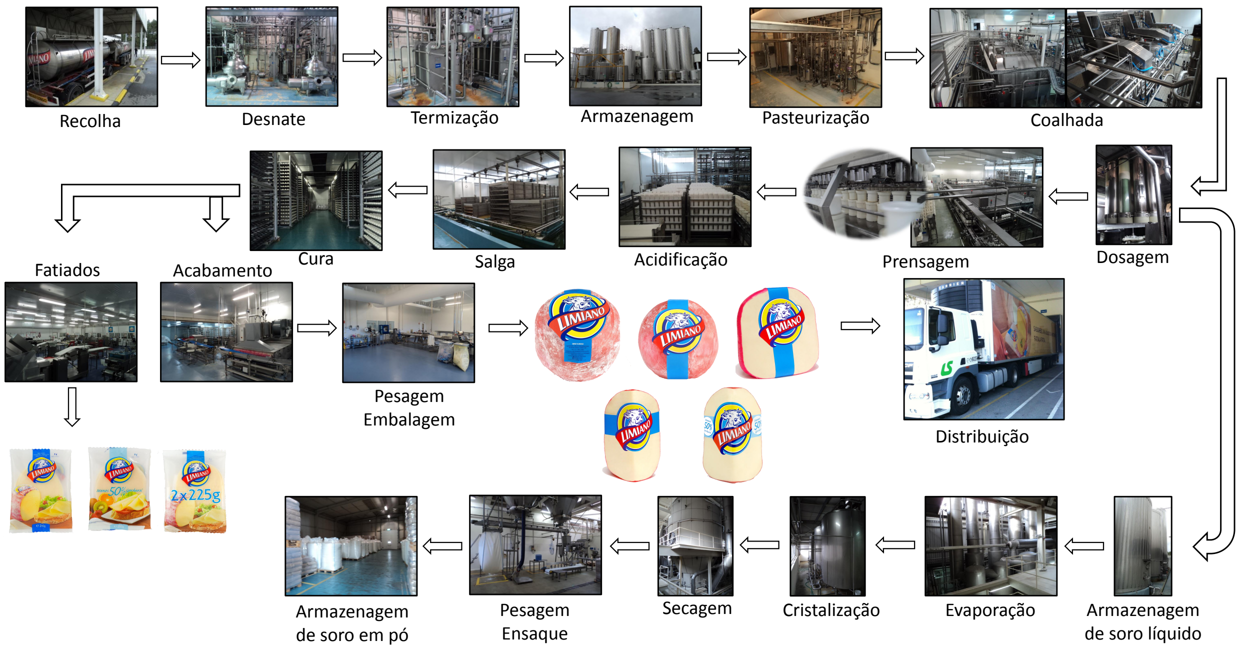

Figure 1.1: Flowchart of BEL Portugal's production process

The company is committed to sustainable operations, implementing strategies to reduce greenhouse gas emissions, optimize energy use, and minimize waste generation. These sustainability principles are embedded in BEL's corporate policy and reflected in its operational decision-making.

The ice water distribution line at BEL Portugal was originally constructed several years ago, with successive additions and modifications to support production growth. However, these expansions were not always accompanied by complete updates to system documentation. As a result:

- Pipeline layouts are partially outdated, leading to potential errors in operational planning and maintenance;
- Unbalanced hydraulic distribution may occur due to changes in system geometry over time;
- Potential inefficiencies in the system could lead to increased energy consumption and temperature control instability;
- Heat gains and pressure losses in certain branches may be impacting overall refrigeration performance.

Given the energy-intensive nature of refrigeration systems in the food industry, these issues have significant operational and economic consequences. Ice water inefficiencies not only raise energy costs but also lead to increased greenhouse gas emissions, directly impacting BEL's environmental footprint and market competitiveness.

By enhancing the reliability and efficiency of the chilled water system, the project strengthens BEL Portugal's operational resilience, supports its sustainability commitments, and creates a technical foundation for future plant expansions and upgrades.

Chapter 2

Literature Review

2.1 Current status

Refrigeration technology is crucial for sustainable industrial operations across various sectors, including food preservation, chemical manufacturing, biomedical storage, and climate control. In the food industry, maintaining product quality, safety, and shelf life throughout production and distribution is crucial, making it a key component of modern industry.

A key infrastructure solution in modern industrial refrigeration is the ice water network, which uses one or more central refrigeration plants to cool a secondary fluid, usually a water or glycol-water mixture, that is circulated throughout the facility. These secondary loops remove the need to circulate primary refrigerants, such as ammonia or hydrofluorocarbons (HFCs), through occupied spaces, thereby lowering the risk of refrigerant leaks and improving worker safety. This method is essential in the food industry, where ammonia continues to be a preferred refrigerant because of its better thermodynamic efficiency, zero ozone depletion potential, and low global warming potential [1].

As a result, ammonia-based central plants with secondary chilled-water loops are now more common in large food processing plants, cold storage warehouses, and supermarket distribution centers. In these designs, ammonia stays in the machinery room. It cools the secondary fluid, which is then pumped to evaporator coils in production halls, storage rooms, or display cabinets.

Nevertheless, despite the operational and safety benefits, ice water networks require significant capital investment for insulated piping, pumping systems, and heat exchangers. Additionally, hydraulic losses and pumping energy can be substantial if networks are poorly designed or oversized.

From an energy perspective, centrally managed ice water networks offer several benefits. They enable load sharing among refrigeration units and improve performance when running at part-load. These networks also support heat recovery, which can be utilized for cleaning, preheating water, or space heating. Despite these benefits, the sector faces operational and environmental challenges. Managing water quality is essential to prevent scaling, corrosion, and microbial growth, especially in open systems. Facilities must also strike a balance between reliability and sustainability.

In summary, ice water systems are poised to become central to the food industry's efforts in safety, sustainability, and energy efficiency. As regulations tighten, focus on designing systems that maximize energy efficiency, facilitate the use of renewable energy, and incorporate advanced monitoring tools to achieve optimal results.

2.2 Latest developments

Chilled-water networks remain a backbone technology for industrial refrigeration in the food sector, and recent research emphasizes making these networks safer, more efficient, and better integrated with energy-management strategies. Modern ice water architectures typically use a primary loop (chillers and condenser/cooling towers) and one or more secondary loops that distribute glycol/water to process heat-exchangers and cold rooms. This separation reduces refrigerant inventory in occupied spaces and simplifies safety compliance in facilities that use potent refrigerants such as ammonia. Recent literature and reviews continue to treat secondary ice water architectures as a best practice for large food-processing plants and distribution centers [2].

Energy optimization and demand-side flexibility are now central research themes. Several recent studies show that ice water networks can act as active thermal storage (using ice water buffers) and be managed with model predictive control or demand-response strategies to shift load away from peak grid prices and renewable intermittency. In simulated food-processing cases, combining ice water buffering with predictive control reduced peak power consumption and overall energy costs while maintaining process temperatures. These strategies are desirable where electricity prices vary or where sites participate in grid flexibility programs [3].

Coupling ice water plants with hybrid and renewable sources is another active area. Hybrid systems that combine electric chillers with waste-heat-driven absorption chillers, solar thermal pre-cooling, or other renewable inputs enable greater fuel and carbon savings while maintaining the reliability required for food safety. Recent hybrid-cooling studies outline retrofit pathways for existing ice water plants, enabling facilities to gradually add low-carbon heat sources without incurring significant downtime [4].

Finally, district and next-generation ice water networks are increasing in popularity in dense industrial parks and food clusters. The “four generations” framework for district cooling indicates a shift toward lower-temperature distribution, higher ΔT operation, and digital integration, all pertinent to future ice water distribution for multiple food industry tenants (central plants offering ice-water-as-a-service). Where available, district ice water provides savings and more efficient plant utilization compared with independent on-site plants. [5].

2.3 Premise of project

The development of this project began under a set of constraints and with several initial challenges that influenced both its planning and early execution.

1. Organization of existing company information:

   A substantial amount of relevant technical information already existed within the company, but it was scattered across various sources and formats. This included old technical drawings of different sections of the ice water line, as well as spreadsheets, graphs, and tables with operational data. The first challenge was to locate, review, and organize these materials in a clear and accessible manner. This process involved identifying discrepancies between documents, verifying outdated measurements, and ensuring the project used the most recent and accurate information.

2. Compilation into a unified system diagram:

   After organizing the available data, the next step was to create a single, detailed drawing of both chilled water lines. This involved on-site measurement of pipe diameters and lengths, as well as identifying and annotating all valves, bends, fittings, and other components that could cause pressure losses in the system. The process also required careful cross-referencing between field observations and existing documentation to ensure accuracy.

3. Learning curve and integration into the company environment:

   Since this project was developed within the company's operational framework, it was necessary to adapt to its internal methods, workflows, and communication channels. This process of integration involved familiarizing oneself with company-specific standards, understanding the technical background of the facilities, and establishing effective collaboration with colleagues from various departments.

4. Review of technical knowledge:

   To ensure the project's quality, it was necessary to review and reinforce certain technical concepts, especially those related to fluid mechanics, pressure drop calculations, and CAD-based technical drawing. This review was crucial for both the design and analytical phases of the work.

The following initial ideas guided the first steps toward developing the project:

- *AutoCAD* modeling:

  The goal was to produce both 2D and 3D representations of the chilled water network. A complete 2D *AutoCAD* drawing was successfully produced, offering an accurate plan view of the system. However, the development of the 3D model was not completed due to technical limitations and compatibility issues with the available software, which hindered the use of certain advanced modeling features.

- Pressure drop calculations:

  A key analytical goal was to quantify pressure losses across the chilled water network. Initial attempts using specialized software failed due to technical issues and unexpected software responses. Therefore, the calculations proceeded manually, using standard engineering equations and empirical measurement data.

Chapter 3

Ice Water Network

3.1 Ice Water Thermal Cycle

Figure 3.1 illustrates a simplified schematic of the ammonia refrigeration circuit that drives the ice water system. The circuit is composed of two condensers, two separators, two compressors, two expansion valves, a liquid receiver (deposit), and an ice bank that functions as the evaporator and as a thermal storage unit.

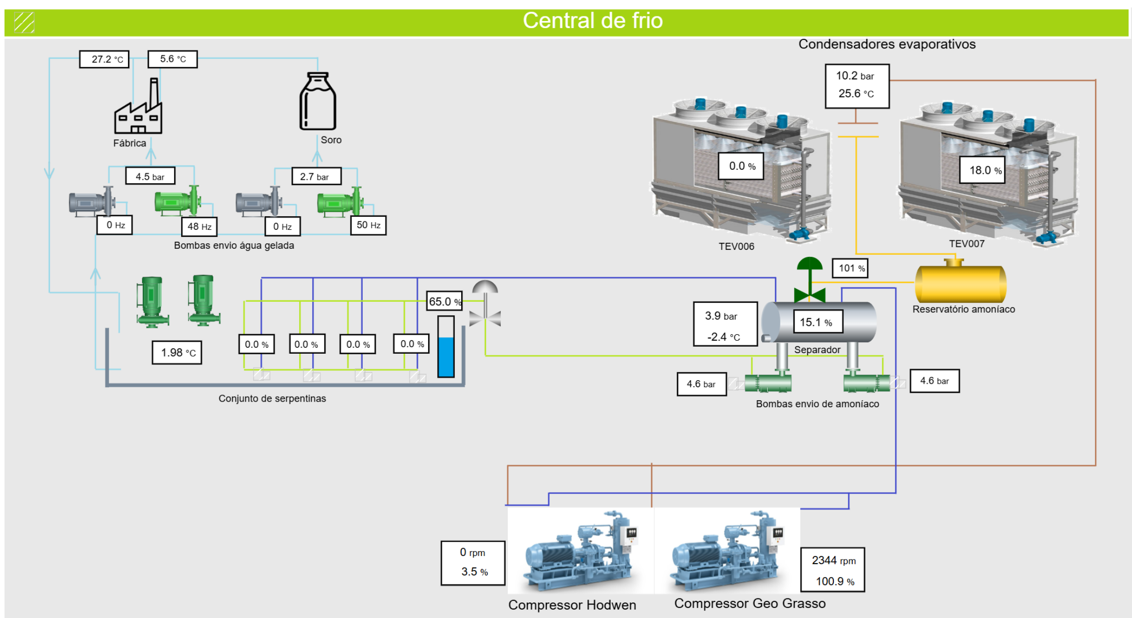

Figure 3.1: Schematic of the ammonia circuit (see Figure A.1 for a more detailed version).

In this configuration, compressors increase pressure to circulate ammonia. Condensers reject heat to the environment. Separators allow only vapor to enter the compressors, protecting them from liquid. Expansion valves control the pressure drop and feed liquid ammonia to the evaporator. The evaporator, in this case the ice bank, absorbs heat from the ice water circuit and freezes water, producing ice for later cooling.

This thermal cycle directly compares to a conventional vapor-compression refrigeration cycle using ammonia. Figure 3.2 shows this. Temperature–entropy and pressure–enthalpy diagrams illustrate compression, condensation, expansion, and evaporation. Storing cooling as ice adds energy storage, increasing flexibility and lowering peak electricity use.

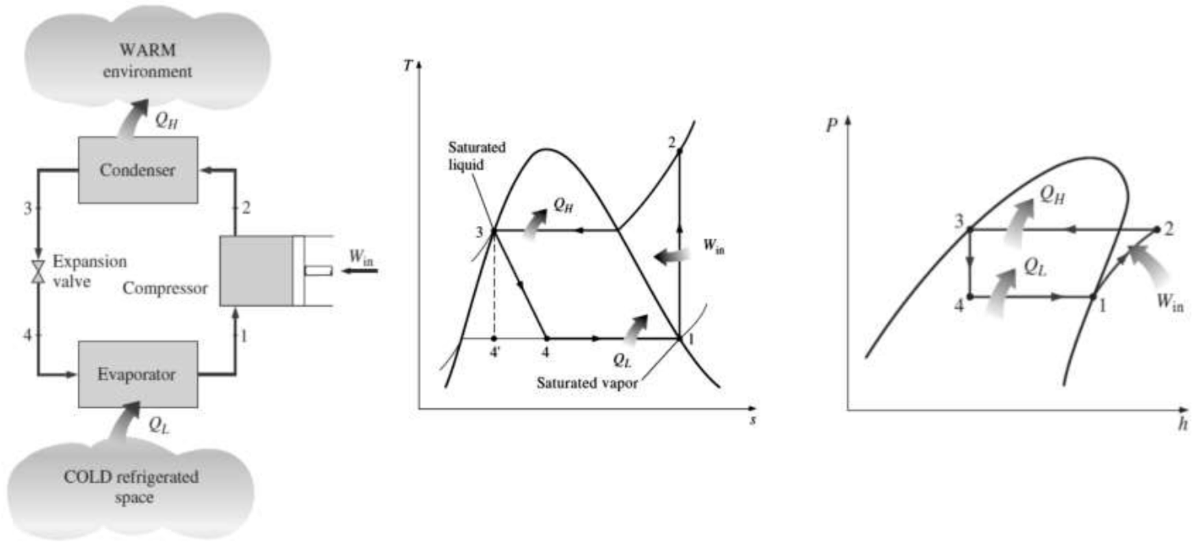

Figure 3.2: Vapor-compression cycle represented in $T{-}s$ and $P{-}h$ diagrams.

3.1.1 Ice Water Tank

In a frozen water thermal storage system, operators produce ice during off-peak hours, when electricity demand and energy costs are lower, by running high-efficiency ammonia refrigeration units. The refrigeration system circulates ammonia through heat exchangers to remove heat from water, gradually freezing it into solid ice. Large, well-insulated ice tanks then store this ice to minimize heat gain and preserve cooling capacity for extended periods.

When cooling is required, especially during peak electricity demand hours, the system circulates the secondary coolant ammonia through serpentine tubing embedded within the stored ice. As the ice melts, it absorbs significant amounts of heat, thanks to the latent heat of fusion, maintaining a stable and low coolant temperature. This chilled water is then distributed to food storage rooms, processing lines, or other temperature-sensitive areas, effectively removing heat from the environment without relying solely on real-time operation of the ammonia compressors.

By moving ice production to off-peak hours, frozen water systems lower the refrigeration system's electrical load during peak periods, saving energy and reducing costs. As ice melts at a steady temperature, the system provides stable cooling, crucial for areas like cold chain storage, meat processing, and dairy facilities.

Beyond cost savings, ice storage offers operational resilience. In the event of a power outage or refrigeration system failure, the stored ice continues to absorb heat passively, buying valuable time to protect stored goods from temperature rise. This backup capacity increases product safety and reduces spoilage risk.

When ammonia refrigeration systems are integrated with frozen water storage, the combination leverages ammonia's high cooling efficiency with the time-shifting and load-leveling benefits of thermal energy storage. This synergy delivers a sustainable and effective industrial cooling strategy, improving energy efficiency, reducing peak demand, and lowering greenhouse gas emissions, while ensuring consistent temperature control to preserve the freshness, quality, and safety of food products in large-scale operations.

3.1.2 Compressors CP1 and CP2

As shown in Figure A.1, the system uses two separate compressors: compressor Hodwen (CP1) and compressor Geo Grasso (CP2). Each compressor operates under different conditions to optimize operational costs and energy usage.

During daytime operation, CP1 provides active cooling to maintain the desired ice water temperature for the facility's needs. Its primary role is to meet the immediate cooling load, ensuring that water circulated to the process or storage areas remains within the required temperature range.

At night, when electricity tariffs are significantly lower, CP2 is activated. During this mode, the system prioritizes maintaining ice water temperature over producing and storing cooling capacity as ice. CP2 operates to form the thickest possible ice layer on the coils immersed in the ice water tank. This ice production phase continues until the coils are coated with the thickest ice layer achievable under design constraints, effectively storing thermal energy for the following day's peak demand period.

In both operational modes, the ice water tank is equipped with heat exchange coils with circulating ammonia refrigerant. The ammonia absorbs heat from the water, either lowering its temperature directly (in daytime cooling mode) or removing enough heat to freeze water onto the coils (in nighttime ice-making mode). This setup uses ammonia's high thermal efficiency and off-peak electricity rates to minimize operational costs.

3.2 Components of ice water line

3.2.1 Pumps of ice water

There are two ice water lines, each equipped with two pumps:

- **Drying Line A – EFAFLU NNJ 50-200/15/2** [6] This line includes two pumps with a total flow rate of around 15 m^3/h. Typically, only one pump operates at a time. As shown in the graphs in Annexes A.2 and A.3, the head (H) is approximately 70 m.

- **Production Line B – LOWARA NSCS 100-200/370/W25VCC4** [7] This line operates with a single pump running of the two as well, delivering a total flow rate of 50 m^3/h. The head (H) is 31 m, as shown in Figures A.2 and A.5. The (NPSHR) is around 5 m, as indicated in Figure A.6 of its catalog.

To ensure a conservative analysis, the flow rate of the pumps was considered at a lower operating value, representing a worst-case scenario for the hydraulic behavior of the network. Under reduced flow conditions, the velocity inside the pipelines decreases, which results in higher pressure drops along the lines. This approach allows for the evaluation of the system under more demanding conditions, ensuring that the design and operation remain reliable and safe even when pumps operate below their nominal capacity.

3.2.2 Properties of the Piping

The chilled water distribution network is composed primarily of galvanized steel piping, selected for its durability, corrosion resistance, and suitability for industrial cooling applications. For heat transfer calculations, the thermal conductivity of the pipe material was taken as:

$$k_{\text{pipe}} = 15 \text{ W/m·K } [8,\ 9].$$

The piping is covered with thermal insulation to minimize unwanted heat gains from the surrounding environment. The insulation material used has a thermal conductivity of:

$$k_{\text{insulation}} = 0.036 \text{ W/m·K } [10].$$

For systems operating at temperatures around 0°C, insulation thickness is recommended to exceed 25 mm in order to ensure adequate thermal resistance and reduce refrigeration loads.

The mechanical insulation, intended for protection against mechanical damage, was considered negligible in heat transfer calculations, as its contribution to the overall thermal resistance is minimal compared to that of the thermal insulation layer (Figure 3.3).

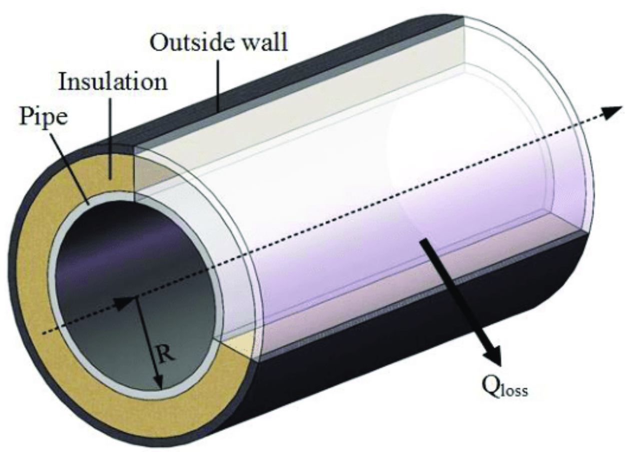

Figure 3.3: Diagram of the different layers of the pipe [11]

The internal roughness of the stainless steel piping was taken as:

$$\epsilon = 0.015 \text{ mm}.$$

3.2.3 Most Common Valve Types and Typical Applications

In fluid distribution networks, particularly in industrial refrigeration, process cooling, and other thermal systems, valves are crucial for controlling, isolating, and directing flow to meet operational and safety requirements. Selecting the appropriate type of valve and actuation method is vital for ensuring system efficiency, reliability, and easy maintenance.

Valves vary not only in their internal design, which determines how they control or block fluid flow, but also in their actuation method, influencing their responsiveness, precision, and suitability for automation. Depending on the application, a valve may be operated manually for simple isolation tasks or automatically through electric, pneumatic, or hydraulic actuation for more complex control functions.

This section describes the most common valve types used in these industrial cooling systems, along with their typical actuation mechanisms and placement within the network.

1. Ball Valves or Two-Port Globe Valves (Manual and Piston Actuation)

   Typical Use: Installed at machine inlets/outlets or to isolate particularly long pipeline branches.

   Purpose: Allows complete shut-off or isolation of a section for maintenance or operational flexibility.

Figure 3.4: Two-Port Globe Valve (Manual actuation)

2. Ball Valves or Three-Port Globe Valves (Manual Actuation)

   Typical Use: Used at machine inlets/outlets when three-way flow routing is required.

   Purpose: Allows complete shut-off or isolation of a section for maintenance or operational flexibility. Easier to remove from the line compared to the two-port valve.

Figure 3.5: Three-Port Globe Valve (Manual actuation)

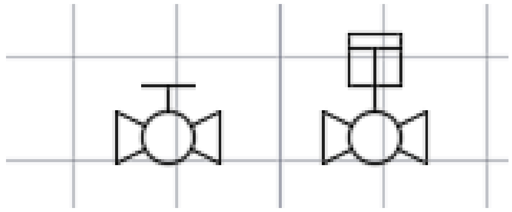

Figure 3.6: Symbols of globe valves, manual and piston, respectively

3. Control Valves (Manual or Solenoid Actuation)

   Typical Use: Used at pump inlets or at the inlets of machines with high flow demand. Occasionally installed on return lines as well.

   Purpose: Regulates flow rate and pressure to match process requirements, ensuring stable system performance.

Figure 3.7: Control Valve (Manual actuation)

4. Control Valves (Diaphragm Actuation)

   Typical Use: Found at machine inlets, outlets, or sometimes both.

   Purpose: Provides smooth and accurate control of flow and pressure, often used where cleanliness and corrosion resistance are important.

Figure 3.8: Control Valve (Diaphragm Actuation)

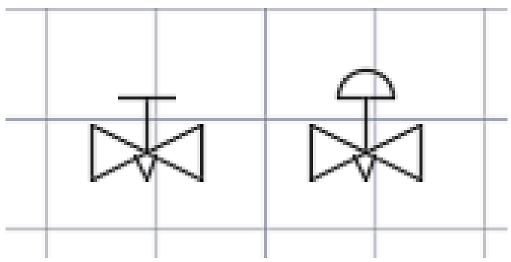

Figure 3.9: Symbols of control valves, manual and diaphragm, respectively

5. Butterfly Valves (Primarily Manual, but also Piston Actuation)

   Typical Use: Installed at the inlets and outlets of new branches, or at machine connections that require relatively low flow.

   Purpose: Offers lightweight, quick shut-off capability with minimal pressure drop for larger diameter lines.

Figure 3.10: Butterfly Valve (Manual Actuation)

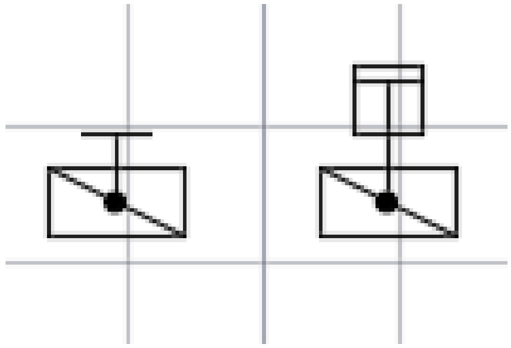

Figure 3.11: Symbols of butterfly valves, manual and piston, respectively

6. Three-Way Control Valves (Manual or Solenoid Actuation)

   Typical Use: Installed in bypass circuits.

   Purpose: Enables flow redirection, system balancing, or temperature control by mixing or diverting fluid paths.

7. Angle Valves (Piston and Solenoid Actuation)

   Typical Use: Located on machine return lines or at the inlet of smaller branches in the system.

   Purpose: Allows a 90° flow turn while controlling or isolating the section, reducing space requirements in compact layouts.

Figure 3.12: Angle Valve (Piston Actuation)

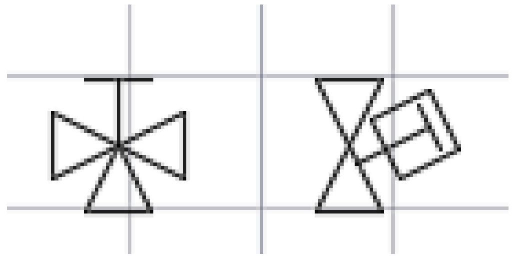

Figure 3.13: Symbols of 3 way control and angular valves, respectively

3.3 Network Layout

In this section, the layout of the ice water distribution network is presented. For each pipeline, a schematic drawing is provided, showing not only the routing of the line but also the points of utilization where the ice water is applied and the type of equipment connected. Each branch of the network is characterized by two circuits: one dedicated to the ice water supply (inlet) and another to the return line.

Line A corresponds to the production area for whey and slicing operations. Line B, on the other hand, supplies the main factory processes.

By analyzing the network structure in this way, line by line, with identification of equipment, supply, and return connections, it becomes possible to obtain a clear understanding of how ice water is consumed throughout the facility and how the refrigeration system supports different production areas.

Figures A.9, A.10, A.11, and A.12 present tables containing the detailed characteristics of each section of the ice water distribution lines. The information includes pipe diameters, total lengths, volumetric flow rates, water velocities, Reynolds numbers (Re), and friction factors (f). These parameters are fundamental for characterizing the hydraulic behavior of the network and for assessing the thermal performance of the system. The compiled data will serve as the basis for the calculations developed in the following chapters, where both the hydraulic analysis and the heat transfer studies are carried out.

3.3.1 Network A

In this part of the network, ice water is primarily used to maintain controlled processing temperatures, ensuring product quality and food safety.

In Figure 3.14, the inlet and outlet connections of the ice water tank are illustrated. The inlet line is directed toward two pumps, which distribute the flow through the network.

After the pumping stage, the flow is divided into two separate branches: one branch supplies ice water to the drying building, while the other is routed to the upper floor, where it serves the sliced cheese processing room.

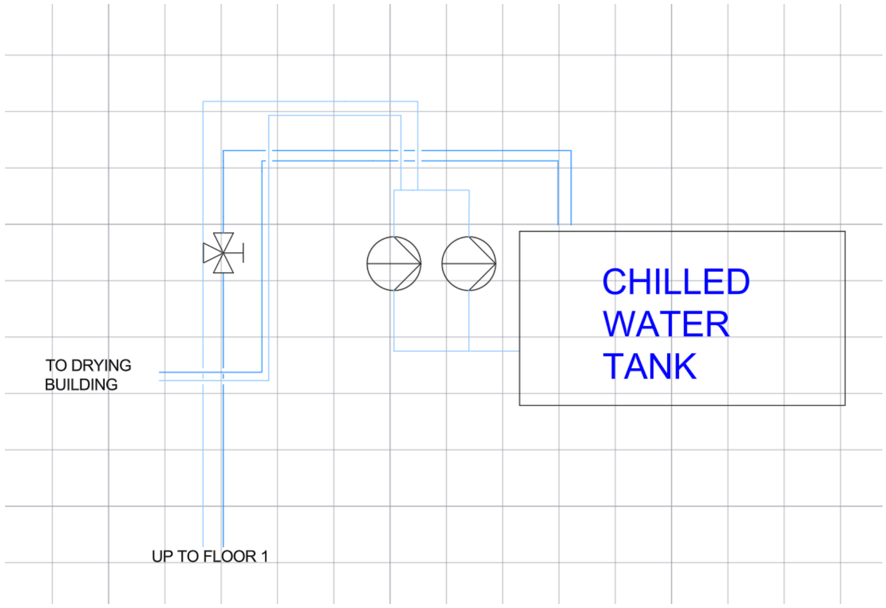

Figure 3.14: Layout of Line A (part 1)

When the line extends to the upper floor (Figure 3.15), the ice water flow is divided into two branches. The first branch remains within the sliced cheese processing room, where it supplies two conditioners dedicated to that area. The second branch continues upward to the roof, where it feeds several units: a drying tunnel and a finishing conditioner for the ball cheese processing room, a conditioner serving the grated cheese processing line, and UTA located in the finishing portions area.

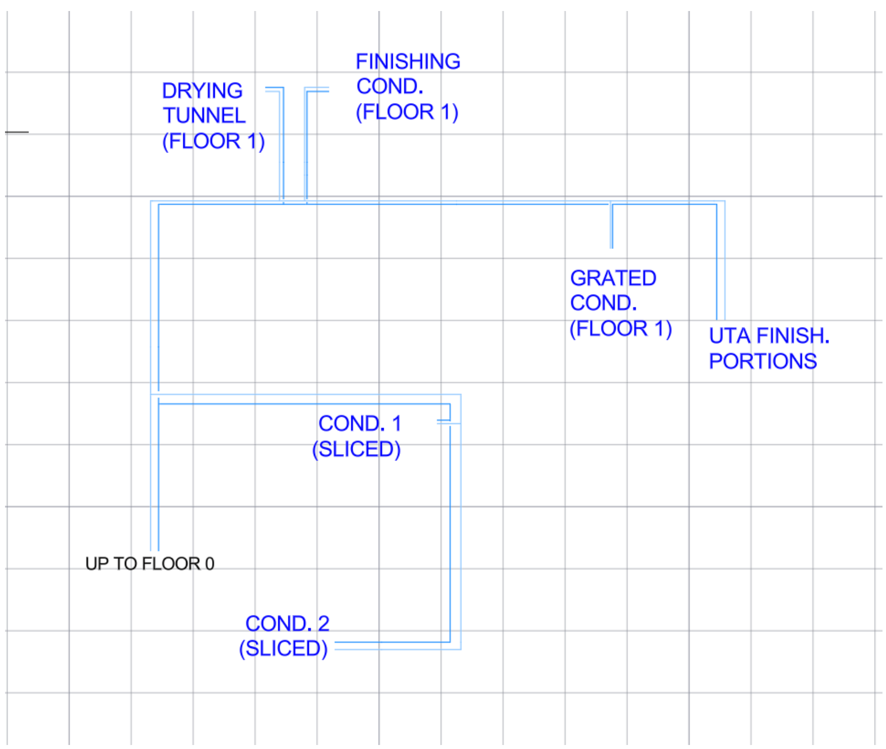

Figure 3.15: Layout of Line A (part 2)

The pipeline supplying the drying building (Figure 3.16) branches into three distinct circuits. The first branch delivers ice water to the crystallizers, ensuring controlled cooling during product formation. The second branch serves the reverse osmosis unit, maintaining stable operating conditions for water treatment. The third branch supplies the drying fan, where chilled water is used to regulate air temperature and support the drying process.

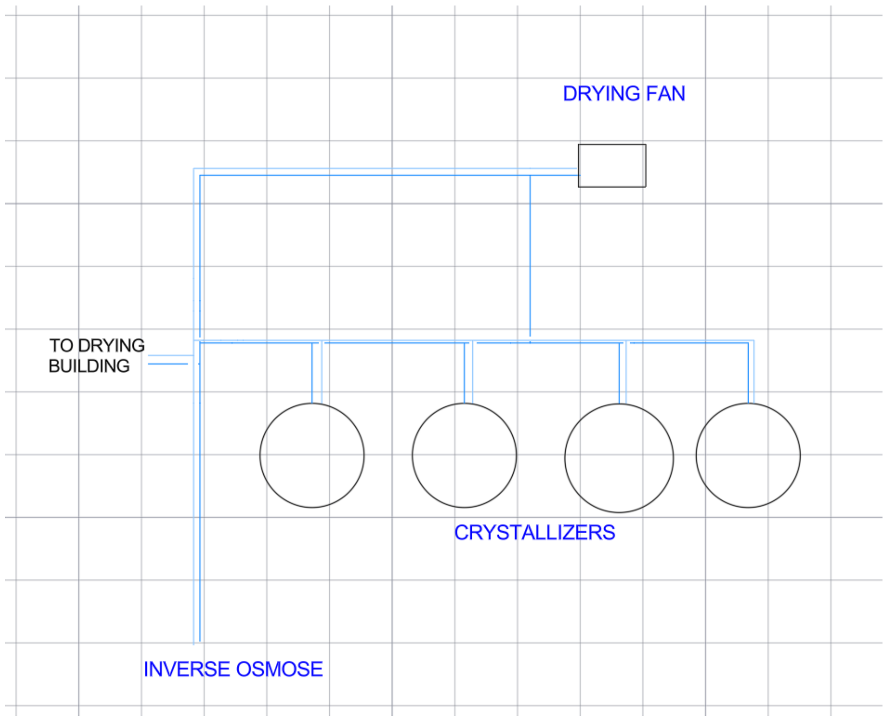

Figure 3.16: Layout of Line A (part 3)

3.3.2 Network B

In Figure 3.17, the inlet and outlet connections of the ice water tank are shown. The inlet line is routed through two circulation pumps, which drive the distribution of ice water throughout the network.

Similar to Network A, the flow is divided into two main branches: one branch supplies the CIP room, while the other is directed upward to feed a lung tunnel located on the upper floor. Additionally, the return line from the manufacturing tanks is combined with the return line of the lung tunnel before re-entering the ice water tank.

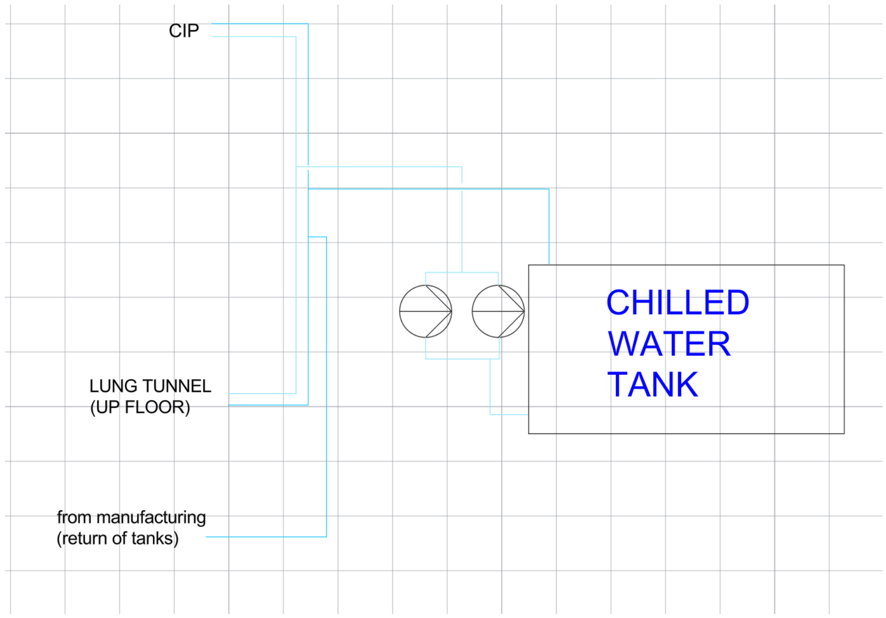

Figure 3.17: Layout of Line B (part 1)

From the CIP room, the ice water pipeline branches into two circuits, as illustrated in Figure 3.18. One branch supplies the thermalization room, ensuring proper temperature control for the process carried out in that area. The other branch serves the cream expedition section, where it cools the cream expedition tank and also provides ice water to a heat exchanger dedicated to cream cooling.

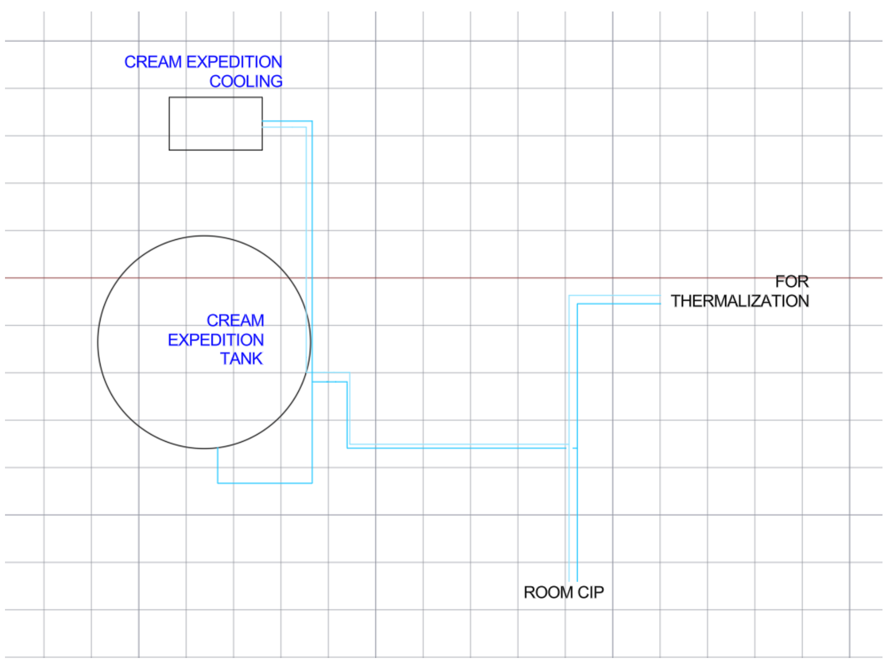

Figure 3.18: Layout of Line B (part 2)

From the lung tunnel, the ice water distribution line is divided into two branches, as shown in Figure 3.19. The first branch supplies the technical floor of the manufacturing area, while the second branch serves multiple units: the cream pasteurization system and its storage tanks, the thermizers, the cream ripener, the creamers, the serum cooling unit, and an air handling unit (UTA). The figure also highlights the point where the line splits from the thermalization circuit, establishing a connection with the CIP distribution line (Figure 3.18.

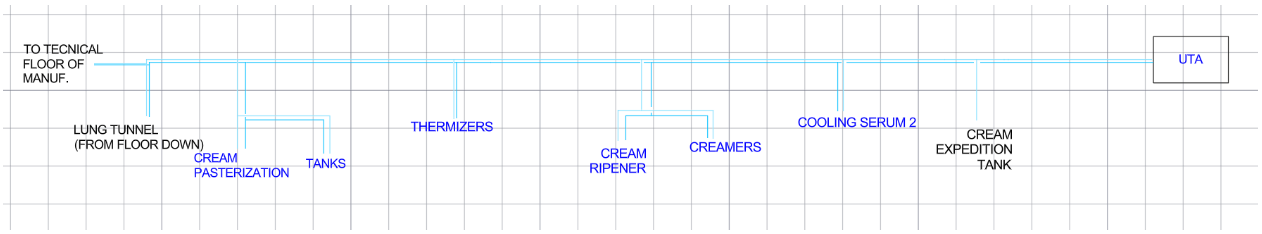

Figure 3.19: Layout of Line B (part 3)

In Figure 3.20, the chilled water distribution on the technical floor of the manufacturing area is shown. At this level, the line supplies two basement conditioners, a heat exchanger used for heating and cooling the changing rooms (currently disabled), a humidifier, the manufacturing air handling unit (UTA), the NAVEP unit (currently disabled), the serpentine tank, and an additional manufacturing conditioner.

From this point, the line extends to the manufacturing floor, where it feeds several process units, including a mass lung tank, a cooling heat exchanger, additional storage tanks, and the Chalon and Tebel Cubos and equipment. The return flow from these tanks is directed downward, connecting directly back to the ice water tank, as illustrated in Figure 3.17.

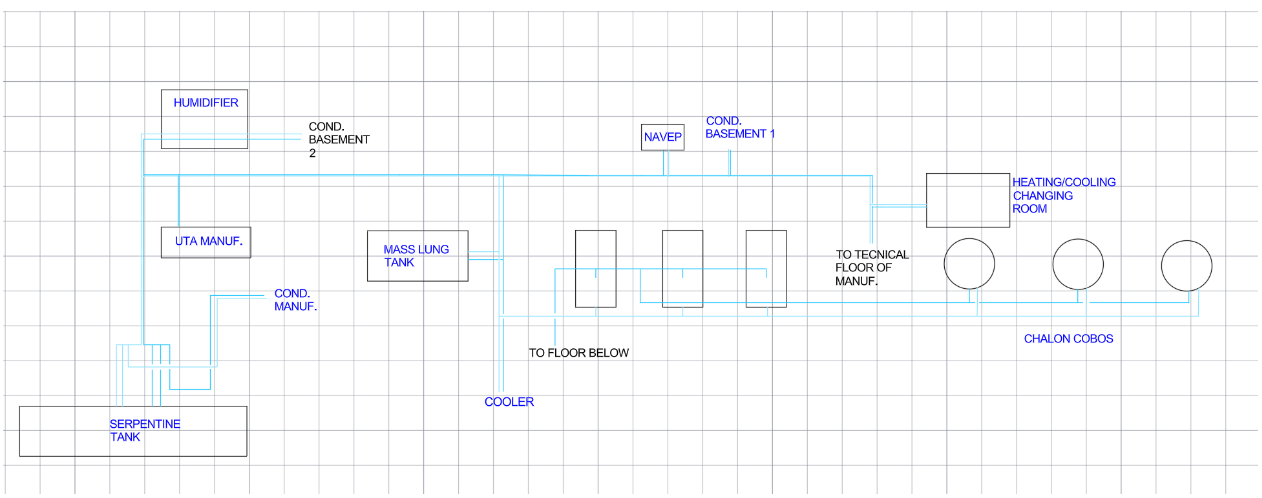

Figure 3.20: Layout of Line B (part 4)

Chapter 4

Hydraulic and Heat Studies of the Site

4.1 Hydraulic study

To assess the hydraulic performance and avoid operational issues such as cavitation, pressure loss calculations were conducted for both ice water lines (See Tables A.1 and A.2 for more detail). The initial pressures at the pump inlets are:

- **Line A:** $P_{A,\text{initial}} = 2.7 - 3.05$ bar
- **Line B:** $P_{B,\text{initial}} = 4.34 - 4.5$ bar

The vapor pressure of water at the operating temperature is taken as $P_v = 900$ Pa.

The pressure drop (Δp) throughout the pipeline is calculated using the following equation [12], which accounts for both frictional losses and local losses:

$$\Delta p = f \cdot \frac{l \cdot \rho \cdot v^2}{2 \cdot D} + k_l \cdot \frac{\rho \cdot v^2}{2} \tag{4.1}$$

Where f is calculated by [12]:

$$f^{-0.5} = 1.8 \cdot \log((\frac{\epsilon}{3.7 \cdot D})^{1.11} + \frac{6.9}{Re}) \tag{4.2}$$

The regions where the pressure drop is most significant typically include:

- Long horizontal stretches with high velocity,
- Bends and elbows, due to abrupt directional changes,
- Valve junctions and other fittings where k_l increases (more information in the Annex A4),
- Narrow sections where velocity increases due to reduced cross-sectional area.

Detailed results and breakdown by sub-sections of pressure drop of the pipeline can be found in the Tables in Appendix A.5 (Tables A.1, A.2, A.3 and A.4).

4.1.1 Local Pressure Losses Analysis

In this section, the values of K_l and h_l for each segment of the chilled water distribution lines are calculated, based on the detailed component data provided in the next Table 4.1:

Table 4.1: Local Loss coefficients of Different Elements

Element	k_l
Globe Valve (open)	10
Angle Valve (open)	5
Control Valve (open)	0,4
Butterfly Valve (open)	0,5
Elbow 90º	0,75
Diameter Reduction	0,4
Top Tee	2,7
Side Tee	4
Right Side Tee	0,6
Special Valve Top	5
3-way Valve	3
Inlet	1

These parameters represent, respectively, the local loss coefficient (K_l), which accounts for pressure losses caused by fittings, valves, elbows, and other singularities, and the corresponding head loss (h_l), expressed in meters of water column.

Determining these values for each section of the network is essential for estimating the total pressure drop across the system, as outlined in the previous section. The calculated results are organized and presented in Tables 4.2, 4.3, 4.4, and 4.5, where each table corresponds to a different branch of the distribution network, 1 corresponding to the inlet branch and 2 to the outlet branch of each line. This Tables represent the sum of the k_l values corresponding to their head loss elements.

Table 4.2: Head Losses by Section A1

Section	Head Loss Elements	K_l	h_l
0	inlet, 2 cuts, 4 elbows, 2 side tees	11.8	0.277
1	control valve, elbow, top tee	4.85	0.52675
2	5 elbows, side tee	7.75	0.21
3	10 elbows	7.5	0.201
4	2 butterfly valves, 6 elbows, control valve, 2 globe valves	25.9	0.1758
5	2 elbows, butterfly valve	2	0.0135
6	top tee, diameter reduction, butterfly valve	3.6	0.008
7	3 butterfly valves, 3 elbows	3.75	0.01309
8	butterfly valve, 3 elbows	2.75	0.0096
9	globe valve, diameter reduction	10.4	0.01
10	2 butterfly valves	1	0.001
11	top tee, 6 elbows, reduction, globe valve	17.6	0.98
12	3 elbows, butterfly valve, control valve	3.15	0.36
13	top tee, 7 elbows, 2 control valves	8.75	0.0066
14	elbow	0.75	0.00014
15	2 elbows, control valve, butterfly valve	2.4	0.016
16	butterfly valve	0.5	0.0039
Total			**2,828**

Table 4.3: Head Losses by Section A2

Section	Head Loss Elements	K_l	h_l
1	12 elbows, side tee, inlet, special valve (top)	19	2.06
2	13 elbows	9.75	0.265
3	2 butterfly valves, 6 elbows, control valve, 2 globe valves	25.9	0.175
4	2 elbows, butterfly valve	2	0.013
5	top tee, diameter reduction, butterfly valve	3.6	0.008
6	butterfly valve, 3 elbows	2.75	0.096
7	2 butterfly valves, 3 elbows	3.25	0.011
8	globe valve, diameter reduction	10.4	0.01
9	2 butterfly valves	1	0.01
10	top tee, 6 elbows, reduction, globe valve	17.6	0.98
11	3 elbows, butterfly valve	2.75	0.32
12	7 elbows, butterfly valve, control valve	6.15	0.0046
13	3 elbows, butterfly valve, globe valve, control valve	13.55	0.0057
14	2 elbows, control valve	2	0.013
15	butterfly valve, 6 elbows	5	0.0
Total			**421.85**

Table 4.4: Head Losses by Section B1

Section	Head Loss Elements	K_l	h_l
0	inlet, 3 elbows, 2 side tees, 2 control valves	11.5	0.72
1	control valve, elbow, top tee	4.85	0.079
2	elbow, side tee	4.75	40.31
3	10 elbows, top tee, 5 side tees, control valve, 4 butterfly valve	32.6	0.53
4	5 elbows	3.75	0.06
5	top tee	2.7	0.04
6	elbow, side tee, control valve	5.15	0.169
7	side tee, 3 controls, angle valve	10.2	0.088
8	side tee, 2 controls, angle valve	9.8	0.084
9	3 globe valves, angle valve	35	1.05
10	side tee, globe valve	14	0.46
11	elbow, control, globe valve	11.15	0.09
12	elbow, control, globe valve	11.15	0.09
13	elbow, 3 side tees, 3 controls valves	13.95	0.263
14	—	0.0	0.0
15	side tee, 3 elbows, control valve	6.65	0.098
16	—	0.0	0.0
17	—	0.0	0.0
18	2 elbows	1.5	0.028
19	4 elbows, 2 butterfly valves, 3 controls valves	5.2	0
20	3 elbows, 5 side tees, top tee, butterfly valve	25.45	0.399
21	9 elbows, 2 butterfly valves, 2 control valves, 3-way valve, angle valve	16.55	0.0072
22	elbow	0.75	0.0017
23	4 elbows, control valve, butterfly valve	3.9	0.0036
24	top tee, 10 elbows, 2 angle valves, globe valve	30.2	0.57
25	5 elbows	3.75	0.0011
26	9 elbows, 2 butterfly valves, control valve	8.25	0.018
27	3 elbows, 3 right-side tees	4.05	0.0008
28	9 elbows, butterfly valve	7.25	0.0058
29	2 elbows, 2 side tees	9.5	0.0095
30	5 elbows, 4 right-side tees, butterfly valve	6.65	0.028
31	8 elbows, 3 top tees	14.1	0.0038
32	6 elbows, control valve, butterfly valve	5.4	0.0004
33	3 elbows, 3 angle valves, control valve, butterfly valve	18.15	0.011
Total			**5,19**

Table 4.5: Head Losses by Section B2

Section	Head Loss Elements	K_l	h_l
1	inlet, 2 elbows, side tee	6.5	0.42
2	10 elbows, top tee, 5 side tee, 3 butterfly valves, 2 control valves	32.5	0.53
3	5 elbows	3.75	0.06
4	top tee	2.7	0.0049
5	2 elbows	1.5	0.049
6	side tee, globe valve	14	0.46
7	elbow, glob valve	10.75	0.0882
8	elbow, glob valve	10.75	0.0882
9	elbow, 2 side tees, 3 control valves	9.95	0.326
10	—	0	0
11	3 elbows, 4 top tees	10.35	0.61
12	2 elbows	1.5	0.028
13	4 elbows, 3 butterfly valves, 3 control valves	5.7	0
14	3 elbows, 5 side tees, top tee, butterfly valve	25.45	0.85
15	9 elbows, 2 control valves, butterfly valve	8.05	0.0023
16	elbow	0.75	0.0017
17	4 elbows, control valve, butterfly valve	3.9	0.0036
18	top tee, 9 elbows, butterfly valve	9.95	0.187
19	5 elbows	3.75	0.0011
20	9 elbows, 2 butterfly valves, control valve	8.15	0.018
21	3 elbows, 3 side tees	4.05	0.0008
22	9 elbows, butterfly valve	7.25	0.0058
23	2 elbows, side tee	5.5	0.0054
24	5 elbows	3.75	0.0003
25	10 elbows, 6 top tees, 2 control valves	24.1	0.0065
26	4 top tees, control valve, 2 elbows	12.7	0.001
Total			**3,76**

4.1.2 Cavitation Verification

To verify the absence of cavitation, the Net Positive Suction Head Available ($\mathrm{NPSH_S}$) must be greater than or equal to the Net Positive Suction Head Required ($\mathrm{NPSH_R}$), provided by the pump manufacturer.

The $\mathrm{NPSH_S}$ is calculated using:

$$NPSH_S = \frac{P_{\text{entry}} - P_v}{\rho \cdot g} + \frac{v_e^2}{2 \cdot g} \tag{4.3}$$

Where:

- P_{entry} is the absolute pressure at the pump inlet,
- P_v is the vapor pressure,

- v_e is the fluid velocity at entry,

Based on the calculations:

- **Line A:** $NPSH_S = 31.14$ m
- **Line B:** $NPSH_S = 45.84$ m

Considering the catalog-specified $NPSH_R = 8$ m for both pump models, the available $NPSH$ values are significantly higher than the required ones. Therefore, cavitation is not expected to occur under these operating conditions.

4.2 Heat Transmission Study

This section presents the heat gain analysis for two chilled water lines in the facility, called Line A and Line B. The total heat absorbed by the water in each line and the respective thermal resistances along the pipeline insulation were calculated.

4.2.1 Initial Conditions and Parameters

The initial and final water temperatures are initially assumed to be:

- Inlet temperature: $T_i = 1.3$°C (see water properties in Appendix A.7)
- Outlet temperature: $T_f = 5.3$°C in line A and $T_f = 27$°C in line B

The ambient temperature of the room is $T_{room} = 22$°C (see air properties in Appendix A.8), and the average exterior temperature is $T_{ext} = 14$°C [13].

The inner initial diameters of the pipelines are:

- Line A: 0.06 m
- Line B: 0.125 m

4.2.2 Thermal Resistance and Heat Transfer to Ambient

The heat loss through the pipe insulation was evaluated using the thermal resistance method (Figure 4.1).

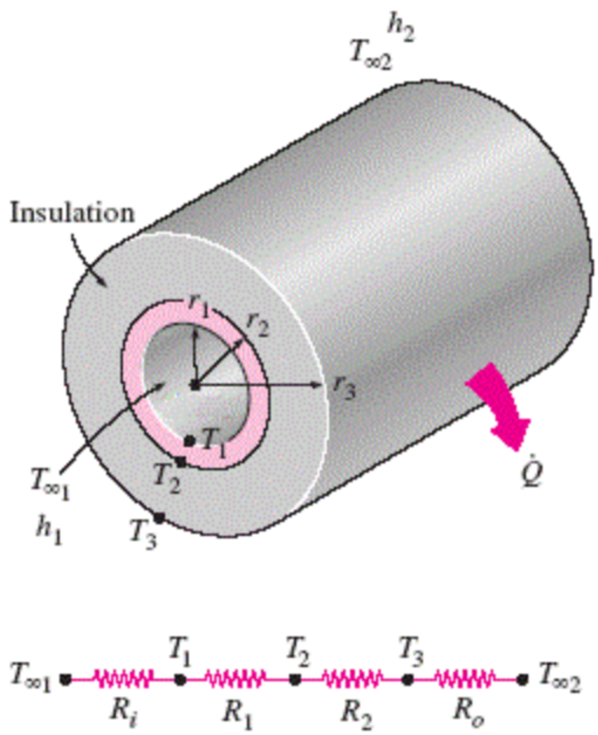

Figure 4.1: Heat Loss in an Insulated Pipe [14]

The total heat transfer (Q_p) to the ambient is given by:

$$Q_p = \frac{T_a - T_e}{\sum R_i} \tag{4.4}$$

Where T_a is the ambient temperature and T_e is the interior temperature of the ice water. The value of T_a depends on whether the specific section of the line is present inside a room (T_{room}) or in the exterior of the factory (T_{ext}). The value of T_e depends if it is calculating the heat transfer inlet (T_i) or the return (T_f). The total thermal resistance is the sum of:

$$R_1 = \frac{1}{2 \cdot \pi \cdot r_i \cdot L \cdot h_i} \quad \text{(Internal convection resistance)} \tag{4.5}$$

$$R_2 = \frac{\ln \frac{r_1}{r_i}}{2 \cdot \pi \cdot k_t \cdot L} \quad \text{(Resistance through tube wall)} \tag{4.6}$$

$$R_3 = \frac{\ln \frac{r_2}{r_1}}{2 \cdot \pi \cdot k_i \cdot L} \quad \text{(Insulation resistance)} \tag{4.7}$$

$$R_4 = \frac{1}{2 \cdot \pi \cdot r_2 \cdot L \cdot h_e} \quad \text{(External convection resistance)} \tag{4.8}$$

Detailed results and breakdown by sub-sections of the pipeline can be found in the Tables in Appendices Tables A.5 and A.7 for inlet, A.6 and A.8 for outlet heat gain.

4.2.3 Convective Heat Transfer Coefficients

The Nusselt number for internal flow (Nu_i) was calculated using the Dittus-Boelter correlation for turbulent flow [14]:

$$Nu_i = 0.023 \cdot Re_d^{0.8} \cdot Pr^{0.4} \tag{4.9}$$

Where:

- Re_d is the Reynolds number:

$$Re_d = \frac{4 \cdot \dot{V}}{\pi \cdot d \cdot \nu} \tag{4.10}$$

- Pr is the Prandtl number.

The internal convective coefficient is then [14]:

$$Nu_i = \frac{h_i \cdot d}{k_{water}} \tag{4.11}$$

For external free convection, assuming horizontal pipe geometry (which dominates the network), the Nusselt number was determined using the Churchill and Chu correlation [14]:

$$Nu_e = \left(0.6 + \frac{0.387 \cdot Ra_D^{1/6}}{(1 + (0.559/Pr)^{9/16})^{8/27}}\right)^2 \tag{4.12}$$

Where the Rayleigh number is [14]:

$$Gr \cdot L_c = \frac{g \cdot \beta \cdot (T_s - T_\infty) \cdot L_c^3}{\nu^2} \tag{4.13}$$

$$Ra_D = Gr \cdot L_c \cdot Pr \tag{4.14}$$

The external heat transfer coefficient is obtained from [14]:

$$Nu_e = \frac{h_e \cdot d}{k_{air}} \tag{4.15}$$

Table 4.6: Calculated thermal parameters for Lines A and B

Parameter	Line A	Line B
Nu_i	397.82	581.727
Re	55015.08	88464.26
h_i	3687.95	2601.48
Nu_e	14.54	27.32
$Gr \cdot L_c$	33607.8	299377.44
Ra	436902.29	3891906.74
h_e	1.868	2.34

Chapter 5

Identification of KPIs and OPIs

In industrial refrigeration, performance must be measured, monitored,, and optimized to ensure reliable operation and energy efficiency. To achieve this, Key Performance Indicators (KPIs) and Operational Performance Indicators (OPIs) are established. KPIs are high-level metrics that measure how well the system meets its core goals, such as energy efficiency and cooling reliability. OPIs, in contrast, are supporting operational metrics that offer insight into daily system behavior and help identify the reasons behind KPI performance.

5.1 Main OPIs

The main OPIs identified for the studied system are the following:

- **Ice Water Temperature** – Continuous monitoring of the supply temperature of ice water ensures that the system is delivering the required cooling conditions to the process. Measured by a temperature sensor, the temperature must generally be between 1.5 and 2.2 ºC.

  Figures 5.1 and 5.2 show the temperature variations of the water leaving the ice water tank over two different time scales: daily and weekly, respectively. The daily profile highlights short-term fluctuations within a single operating day, while the weekly profile shows broader patterns across multiple days of production.

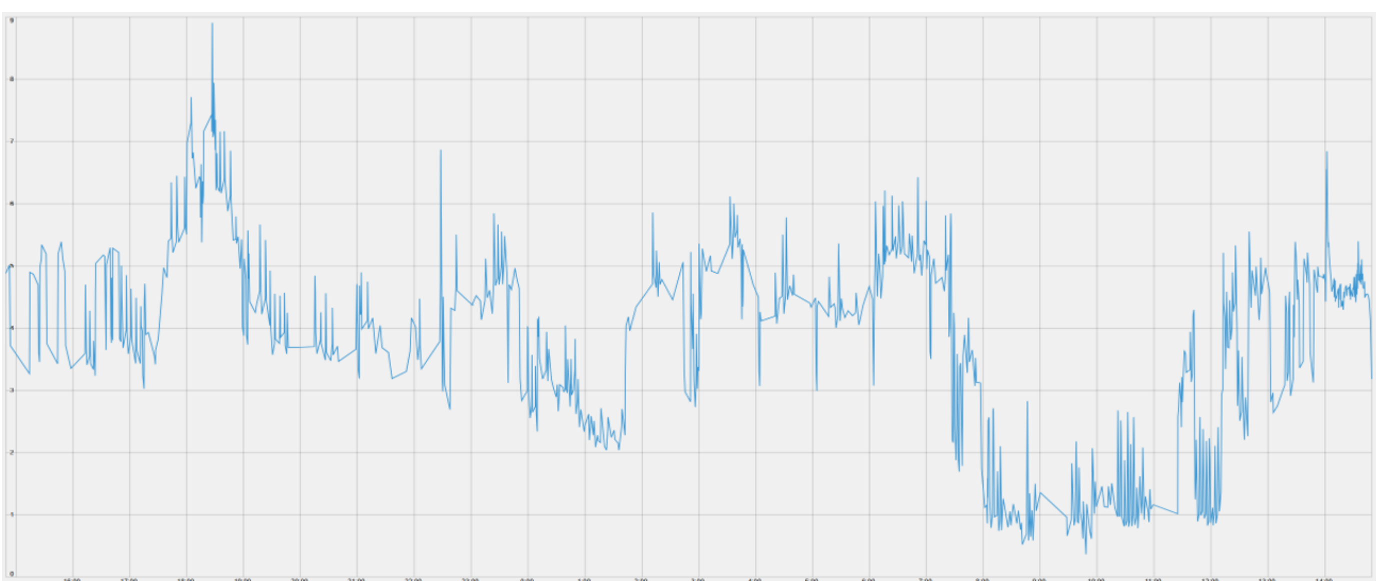

Figure 5.1: Temperature of inlet water in a day

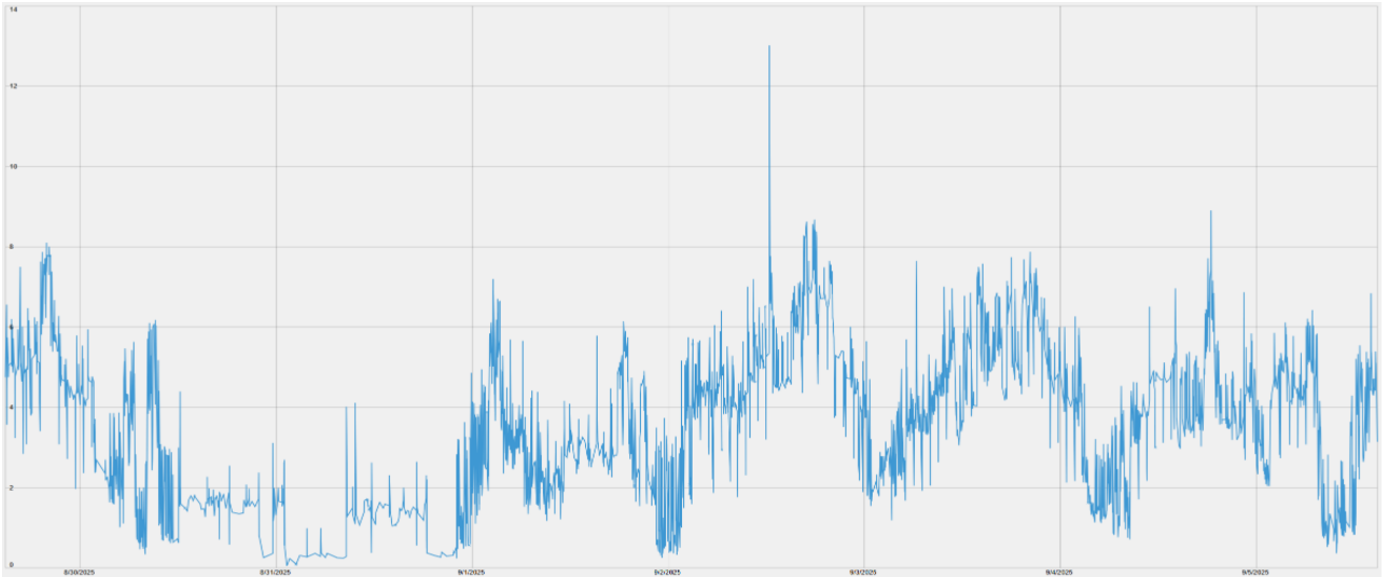

Figure 5.2: Temperature of inlet water in a week

These results show that at certain times of the day, the system operates under standard cooling loads, while at others, the demand increases significantly, requiring higher refrigeration capacity, which results in a higher temperature exiting the chilled water tank.

- **Compressor Suction Pressure** – Indicates evaporator performance and load conditions. Abnormal values may point to fouling, low refrigerant charge, or flow restrictions. This value was measured to be 3 bar.

- **Compressor Discharge Pressure** – Provides information about condenser performance. Elevated discharge pressures may indicate scaling, poor heat rejection, or insufficient cooling water flow. This value was measured to be 11 bar.

- **Compressor Oil Temperature** – Ensures proper lubrication and cooling of compressors. High oil temperatures can indicate mechanical stress or inadequate cooling. Measured by a temperature sensor, this temperature must be around 60ºC.

- **Filtration Time** – Tracks the time required for water filtration, useful to assess water quality and maintenance needs of filtration systems. This value has the objective of 240 minutes.

- **Volume of New Network Water** – Measures the amount of fresh water introduced into the system, which can highlight leakages, excessive makeup water demand, or purges. The objective is to prevent the introduction of new network water into the system, but the value tends to be about 3 m^3.

- **Ice Thickness** – Represents the progress of ice formation in the ice bank and is directly related to available stored cooling capacity. This value tends to be around 20 to 30 mm, depending on the time of day.

- **Compressor Consumption** – Electrical energy consumption of compressors, directly linked to operational cost and system load. The electrical energy consumption of both compressors is:
  - Compressor CP1: 160 to 250 kW
  - Compressor CP2: 433 to 677 kW
- **Factory Supply Pressure** – Pressure delivered to the production areas, ensuring sufficient flow and stable operation in process equipment. This value tends to be around 4.5 bar.
- **Drying Line Supply Pressure** – Pressure at the supply of the drying building, confirming that cooling demand for air-handling or drying processes is met. This value tends to be around 3 bar.
- **Ice Bank Level** – Indicates the available storage capacity of the ice tank and helps manage load shifting between peak and off-peak hours. An ideal operating condition is to maintain the ice bank level above 60 percent, ensuring sufficient stored cooling capacity for peak demand periods.
- **Factory Return Temperature** – Temperature of water returning from the factory processes, useful to evaluate the effectiveness of heat exchange in production. This value tends to be between 8 and 14ºC, with some noteworthy spikes up to 30ºC, especially in days of great frigorific capacity necessities (See Figures 5.3 and 5.4).
- **Drying Return Temperature** – Return water temperature from the drying building, providing insight into the cooling load of drying processes. This value tends to be between 2 and 10ºC, with some noteworthy spikes above those levels, especially on days of great refrigeration capacity necessities.

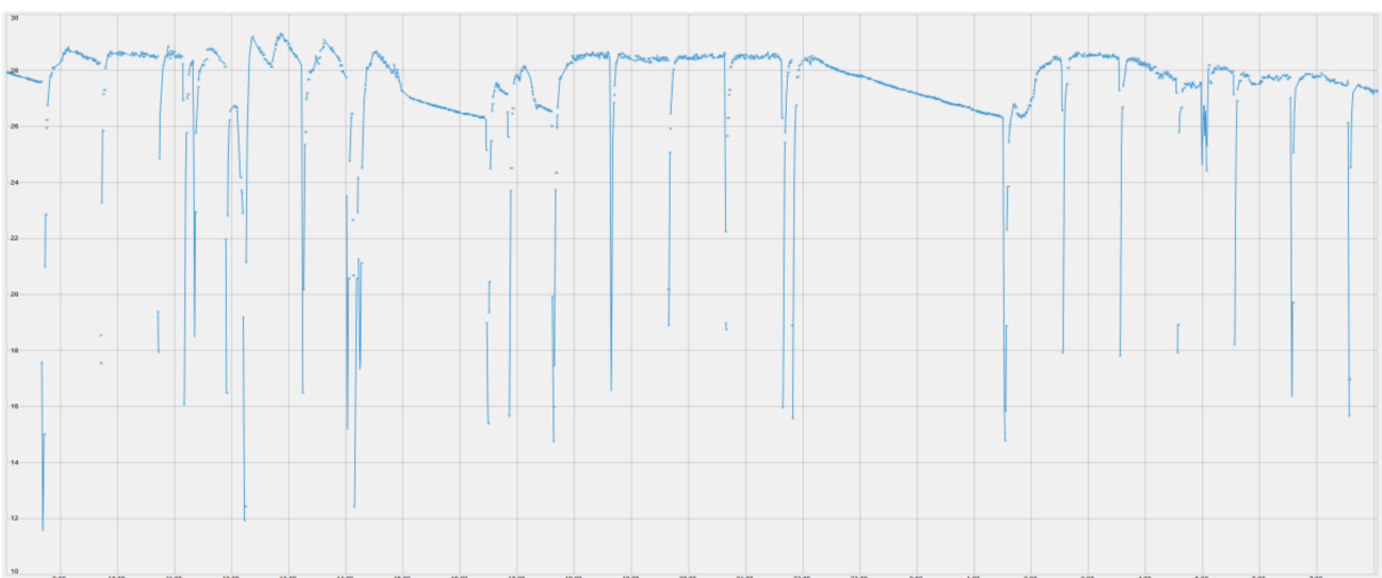

Figure 5.3: Temperature of outlet water in a day

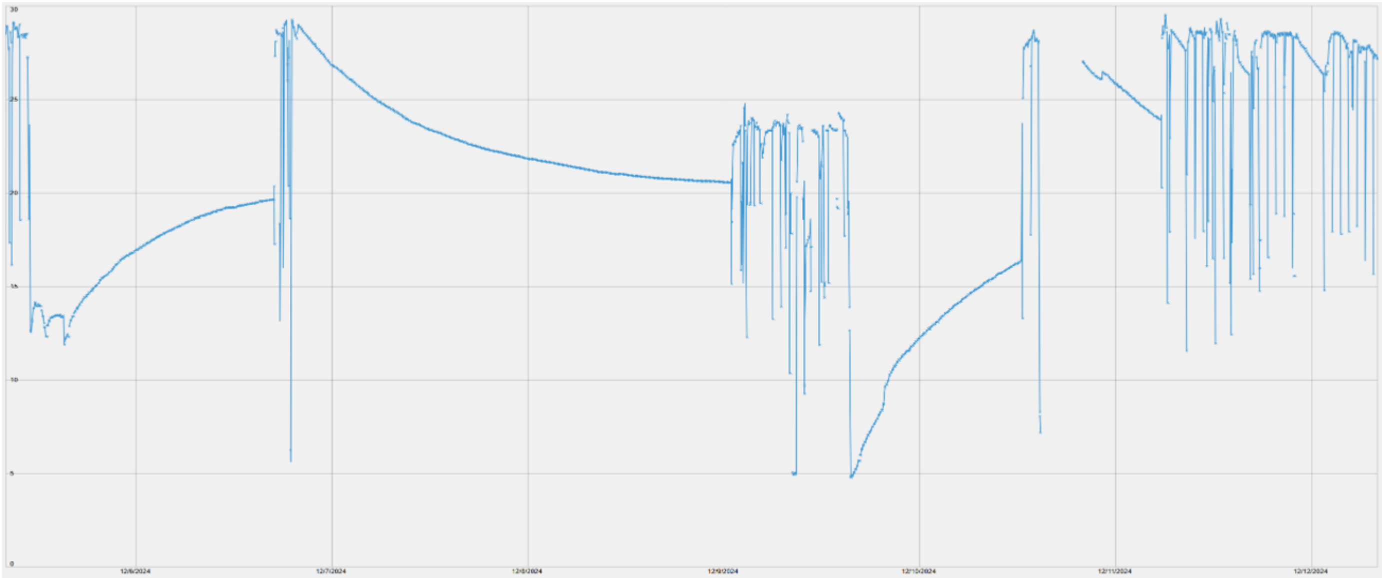

Figure 5.4: Temperature of outlet water in a week

Monitoring these OPIs enables operators to detect anomalies, optimize operating strategies, and ensure that KPIs such as system efficiency, pressure stability, and energy savings are achieved. Together, they form the operational backbone of a reliable and efficient ice water network and central chiller plant.

5.2 Main KPIs

To evaluate the performance of the ice water network and the central refrigeration plant, a set of KPIs is defined. These indicators quantify energy efficiency, productivity, and equipment reliability, providing a clear framework for monitoring and decision-making. Together, these KPIs offer a comprehensive evaluation framework, combining energy efficiency (COP, kWh/TR, kWh/ton of cheese) with equipment reliability and availability (Compressor Availability, MTBF, MTTR). This dual perspective ensures that both operational performance and long-term system sustainability are considered.

5.2.1 COP

- The **Coefficient of Performance (COP)** of the central refrigeration plant measures the ratio between the cooling energy delivered and the total electrical energy consumed by compressors and auxiliaries:

$$COP_{central} = \frac{Q_{cooling}}{W_{total}}$$

where $Q_{cooling}$ is the useful cooling capacity [kW] and W_{total} is the total electrical power input [kW].

By combining the measured temperature variations, it is possible to estimate the frigorific capacity requirements using the fundamental energy balance equation:

$$Q = \dot{V} \cdot \rho \cdot c_p \cdot (T_f - T_i) \tag{5.1}$$

where Q is the cooling capacity, $\dot{V}$ is the volumetric flow rate of water, ρ is the water density, c_p is the specific heat capacity, and $(T_f - T_i)$ represents the temperature difference between the outlet and inlet.

The results of this calculation are presented in Figure 5.5, which displays the hourly profiles of outlet temperature, inlet temperature, and cooling capacity. From these graphs, it is possible to clearly identify the peak demand, as well as the typical times at which these peaks occur. A more detailed breakdown of these results is provided in Annex A.7.

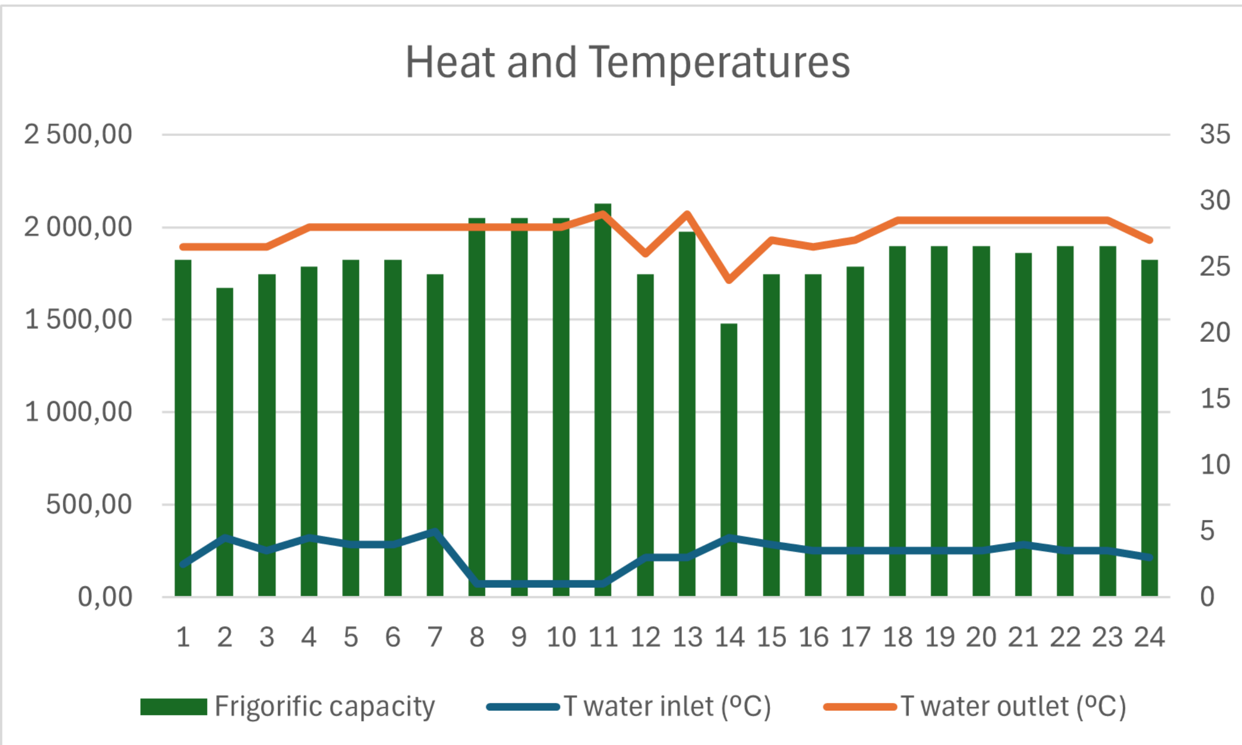

Figure 5.5: Frigorific Capacity Requirements in a day

The main consumers of ice water in the facility include the serum cooling system, cream cooling, multiple air conditioning units (UTAs), several conditioning units, the reverse osmosis system, thermalization, pasteurization, the cream expedition process, and the Chalon and Tebbel cube production lines.

The W_{total} will be the sum of the maximum compressor consumptions :

$$W_{total} = W_{CP1} + W_{CP2} = 927 kW \tag{5.2}$$

The results of the COP calculations indicate that the system operates with a maximum COP of 3.37, a minimum COP of 2.16, and an average COP of 2.63, depending on the refrigeration capacity requirements at the given time. These values demonstrate that the system occasionally reaches the desired operational target of 3–6, but on average, it performs below the ideal range.

The relatively low average COP indicates inefficiencies in the chilled water network and central plant, potentially linked to high pressure drops, suboptimal flow distribution, or excessive heat gains during production. Therefore, improving system design—such as optimizing load distribution and implementing pre-cooling strategies for high-demand processes—could significantly enhance energy efficiency and bring the system closer to the target COP range.

5.2.2 SEC

The **Specific Energy Consumption (SEC)** per refrigeration ton is a key performance indicator (KPI) that measures the electrical energy used for each ton of refrigeration produced. It offers a clear measure of system efficiency, allowing comparisons across different operating conditions or facilities. The SEC is defined as:

$$SEC_{TR} = \frac{E_{consumed}}{TR}$$

where $E_{consumed}$ is the total electrical energy consumption of the compressors $[kWh]$, and TR is the refrigeration load expressed in tons of refrigeration ($1\,TR = 3.517\,kW$).

For the system under study, considering an average refrigeration load of 1844.72 kW and a compressor energy consumption of 927 kW, the resulting SEC is:

$$SEC_{TR} = \frac{927}{\frac{1844.72}{3.517}} \approx 0.173\,\text{kWh/TR}$$

According to industry benchmarks, efficient refrigeration systems typically operate in the range of 0.18–0.25 kWh/TR, with best-in-class systems approaching values close to 0.15 kWh/TR. The obtained value of 0.173 kWh/TR places the studied system within the high-performance range, demonstrating above-average efficiency.

While the target for industrial refrigeration systems is typically a COP between 3 and 6, the correspondence between a low SEC (0.173 kWh/TR) and a moderate COP (2.63) suggests that the system operates efficiently in terms of energy per ton of refrigeration, but there is still room for improvement in thermodynamic performance.

5.2.3 Central refrigeration plant Availability

- The **Availability** measures the proportion of time that the plant is operational and capable of meeting demand:

$$Availability = \frac{MTBF}{MTBF + MTTR}$$

where $MTBF$ is the Mean Time Between Failures [minutes], and $MTTR$ is the Mean Time To Repair [minutes].

- Mean Time Between Failures (MTBF): this KPI quantifies the expected average operational time between two consecutive failures:

$$MTBF = \frac{Total\ Operating\ Time}{Number\ of\ Failures}$$

- Mean Time To Repair (MTTR): this KPI measures the average time required to restore equipment to operational condition after a failure:

$$MTTR = \frac{Total\ Repair\ Time}{Number\ of\ Failures}$$

The reliability analysis was based on the definition of failures as the number of occurrences in which the chilled water supply line temperature exceeded the limit of $3\,°C$. For each month, the total operating time was considered as:

$$\text{Total Operating Time} = 24 \times 60 \times 30 = 43200\ \text{minutes/month}.$$

This reference time was used together with the number of failures to determine the MTBF. Table 5.1 summarizes the values obtained for each month.

Table 5.1: Failures, MTBF, Revisions, MTTR and Availability per month

Month	Nº of Failures	MTBF (min)	Revisions (hours)	MTTR (min)	Availability
January	2	21600	16	480	0.978
February	0	–	8	–	1
March	6	7200	24	240	0.967
April	21	2057.14	6	17.14	0.991
May	14	3085.71	8	34.29	0.988
June	79	546.84	16	12.15	0.979
July	68	635.29	56	49.41	0.927
August	82	526.83	8	5.85	0.988

At the reliability level, indicators such as availability, MTBF, and MTTR quantified the robustness of the system and provided guidance for maintenance planning. The analysis revealed significant variability in performance throughout the months.

These results highlight the existence of critical periods with high failure frequency and reduced reliability, reinforcing the importance of targeted maintenance strategies, prioritization of critical months, and operational adjustments to enhance system robustness.

Chapter 6

Discussion of Results

The results obtained from the thermal and hydraulic studies of the ice water network enable a comparison of heat gains in the distribution lines with the thermal loads linked to the production processes. Additionally, the hydraulic analyses revealed opportunities to redesign parts of the network to improve efficiency in terms of both pressure drop and thermal performance. Moreover, specific equipment, such as the serum cooling system, was identified as requiring additional capacity, leading to the proposal of new solutions. This chapter discusses these findings and their implications for system performance.

6.1 Impact of Inlet Temperature on System Performance

One of the key observations from the analysis is that the inlet temperature of the ice water line is higher than expected, mainly because of increased cooling demands from several processes. This condition spreads throughout the system, as a higher inlet temperature inevitably results in a higher outlet temperature. The consequence is a compounding effect: the system must operate with a greater temperature lift, causing compressors to work harder to deliver the same cooling capacity.

This phenomenon has a direct negative impact on the COP. Since COP is defined as the ratio between the cooling effect produced and the work consumed by the compressors, an increase in both inlet and outlet temperatures results in higher compressor consumption and a reduced effective cooling capacity.

The implications of this behavior are significant. Not only does it increase the operational cost of the refrigeration system, but it also reduces the overall efficiency of the facility. Addressing this issue requires a dual approach:

- **Network optimization:** Reducing unnecessary heat gains in the lines by improving insulation and minimizing line lengths where possible.
- **Process adaptation:** Segregating circuits according to their cooling temperature requirements to avoid overloading the central system with high inlet temperatures.

By reducing the excessive inlet temperature increase, it is possible to stabilize outlet temperatures and improve the cycle's thermodynamic efficiency, therefore increasing COP and decreasing compressor energy consumption.

6.1.1 Heat Gain in Distribution Lines vs. Production Loads

Calculations indicate that the heat gained in distribution lines is only a small fraction of the overall thermal load compared to the heat absorbed during production processes. In practice, this means pipeline inefficiencies do not significantly affect the global energy balance of the refrigeration system.

Based on these findings, the main recommendation is to focus efficiency improvements on reducing heat introduced by production equipment and processes. Pipeline heat gains are less significant and can be addressed as a secondary concern.

6.1.2 Opportunities for Network Redesign

Despite the relatively small heat gains in the lines, the hydraulic study highlighted that the current network layout could be optimized to reduce pressure drop. The present design involves long pipeline routes, which increase frictional losses and therefore pump energy consumption. Redesigning the lines to minimize travel distances between the ice water tank and the production equipment would decrease overall head losses, improving efficiency and reducing operational costs.

In addition to optimizing pipeline routes, another significant redesign opportunity relates to separating lines based on the chilled water temperature required by each production area. Currently, the same supply line serves equipment with varying thermal requirements. This configuration not only complicates control but also leads to situations where water must be cooled more than strictly necessary for some processes. By creating parallel lines with different supply temperatures tailored to each group of processes, it would be possible to reduce unnecessary cooling and associated energy costs.

6.1.3 Opportunities for Cooling Central Redesign

The analysis of return temperatures in the chilled water network showed that Line B consistently has higher return water temperatures than Line A. This indicates that Line B is a strong candidate for a heat recovery or heat exchange solution. Installing a dedicated heat exchanger in Line B's return section would recover excess thermal energy before it re-enters the central system, reduce the compressor load, and improve overall system efficiency.

Another key observation involves regulating the ice bank's operating temperature. The outlet temperature of chilled water should match the lowest process temperature requirement among the connected production lines. By providing a supply temperature suitable for the most demanding process, the system can effectively serve all other processes without overloading the central plant. This approach fulfills thermal requirements while preventing unnecessary overcooling.

It was also found that Line B demands lower inlet temperatures than Line A. To address this, it is proposed to install a dedicated falling film heat exchanger directly at the outlet of the ice bank feeding Line B. In this configuration, the chilled water temperature can be accurately adjusted to meet process needs, avoiding unnecessary overcooling during the entire cycle. This solution ensures that sensitive processes in Line B receive the required low temperatures while maintaining overall system efficiency and preventing excessive energy consumption.

In summary, it is recommended that Line B have a tailored thermal management strategy. This should include a heat exchanger on the return to reduce re-entry temperatures, careful regulation of the ice bank outlet temperature, and prioritization of low inlet temperatures to meet the needs of falling film exchangers and other critical equipment. Implementing these measures will directly improve energy efficiency, stabilize COP, and increase the reliability of production processes dependent on Line B.

6.1.4 Serum Cooling Capacity

One of the most critical results identified is that cooling capacity in the serum cooling process requires a higher thermal capacity relative to other processes. To address this, the installation of an intermediate chiller upstream of the serum cooler is proposed.

This configuration would act as a pre-cooling stage, reducing the temperature of the serum before it reaches the main refrigeration system. It works similarly to cooling a product with cold air prior to placing it in a cold chamber: by reducing the initial thermal load, the strain on the main system is decreased, and overall efficiency is enhanced.

6.2 Summary of Findings

The discussion of results leads to three main conclusions:

- Heat gain in the distribution lines is relatively small compared to the thermal loads from production processes; therefore, efficiency measures should prioritize production cooling.
- Redesigning the network and cooling central can reduce frictional pressure losses and allow for better thermal management by separating lines according to chilled water temperature requirements.
- The serum cooling step represents a critical load, and its performance can be enhanced through the installation of a dedicated pre-cooling chiller.

These findings highlight where improvements will have the most significant impact, guiding future interventions to maximize energy efficiency and system reliability.

Chapter 7

Conclusions and Future Work

7.1 Conclusion

The present work addressed the detailed study of the ice water network and the central refrigeration plant of the industrial site. The main objectives were to analyze the thermal and hydraulic performance of the system, to quantify the heat loads generated by the production processes, to evaluate the pressure drops in the distribution lines, and to establish both Key Performance Indicators (KPIs) and Operational Performance Indicators (OPIs) capable of characterizing the overall efficiency and reliability of the facility. The methodology combined theoretical studies, data collection, thermodynamic and hydraulic calculations, and the structuring of performance indicators into a coherent monitoring framework.

7.1.1 Thermal performance assessment

The thermal analysis of the site demonstrated the importance of matching production schedules with the refrigeration capacity available from the ice water and frozen water systems. Hourly monitoring of the cooling demand for each machine revealed periods of peak consumption, during which the use of stored cooling in the ice bank proved crucial to guarantee system stability.

The comparison between heat loads from the equipment and heat transmission through the piping system confirmed that distribution losses, although secondary to process loads, can still represent a significant share of total energy demand if not adequately controlled. In particular, temperature fluctuations at the outlet of the ice water tank underscored the need for precise control strategies and insulation improvements.

7.1.2 Hydraulic study

The hydraulic study quantified pressure drops in each section of the ice water distribution network. Based on data from Annex A.4, friction and local losses were calculated for all network branches.

Results showed certain sections are more critical, particularly those with multiple control or butterfly valves or frequent directional changes. Analysis of low-flow scenarios highlighted the need to design for worst-case conditions, as reduced velocities can cause unfavorable pressure profiles. This analysis validates pump sizing and identifies optimization opportunities.

7.1.3 Key and Operational Performance Indicators

Defining KPIs and OPIs was a key project outcome, providing measurable variables for long-term efficiency assessment and short-term operational monitoring. These indicators allowed a structured evaluation of the chilled water network and central refrigeration plant, highlighting strengths and areas needing improvement.

At the strategic level, KPIs such as the central COP and SEC established a direct link between energy use and productivity. The results demonstrated that, while the system achieves a competitive SEC of 0.173 kWh/TR, which positions the system within the high-performance benchmark range, the average COP of 2.63 remains below the ideal target of 3 to 6. This discrepancy indicates that, despite good energy efficiency per unit of cooling, thermodynamic performance is limited by operating conditions such as high inlet and outlet temperatures in the lines.

At the reliability level, MTBF, MTTR, and availability quantified system robustness and guided maintenance planning. Results showed substantial variability: January recorded the best performance, while August had the lowest MTBF but still high availability due to short repair times. July stood out with the lowest availability, despite a higher MTBF, reflecting long repair durations. On average, the system presented 45.3 failures/month, an MTBF of 960 minutes, and availability above 96 %. These findings underscore the need for targeted maintenance in critical months.

At the operational level, OPIs such as chilled water temperature, suction and discharge pressures, oil temperature, ice bank level, and return water temperatures support real-time performance monitoring and early detection of inefficiencies. Persistently high inlet water temperatures were shown to propagate through the network, raising outlet temperatures and increasing compressor workload, which in turn lowered COP.

7.1.4 Main conclusions

From the work carried out, the following conclusions can be highlighted:

- The ice water network has the capacity to meet current cooling demands, but optimization opportunities exist in both thermal and hydraulic domains.
- The ice bank is essential for shifting loads from peak to off-peak hours, and its efficient operation requires maintaining an ice level above 60%.
- Heat gains in poorly insulated sections of piping contribute to fluctuations in outlet temperature and should be mitigated through improved insulation.
- Pressure drops are concentrated in sections with complex valve arrangements; their impact can be reduced through optimized network design and valve selection.
- The proposed KPIs and OPIs provide a comprehensive set of tools for monitoring energy efficiency, reliability, and operational stability.

In summary, the project successfully fulfilled its objectives by producing a complete thermal and hydraulic characterization of the chilled water network, by establishing a performance monitoring framework, and by identifying areas where improvements can generate significant efficiency gains.

7.2 Future Works

Although the objectives defined for this work were achieved, further developments are recommended to enhance the results and support decision-making for future investments. Building on the findings discussed in the previous chapter, the most relevant future works include:

- **Network redesign:** Redrawing parts of the chilled water distribution network to minimize pipeline length and, consequently, frictional pressure losses. This redesign should also consider separating lines according to the chilled water temperature required by each production process, allowing for more efficient thermal management and energy savings.
- **Insulation improvements:** Experimental studies to quantify the effect of additional insulation layers on heat gain reduction, with subsequent cost–benefit analysis to guide investment decisions.
- **Serum cooling capacity:** Installation of a dedicated pre-cooling chiller upstream of the serum cooler. This measure would reduce the thermal load entering the main refrigeration system, improving efficiency and ensuring that this critical step operates under stable conditions.
- **Return heat exchanger in Line B:** Evaluation of installing a heat exchanger in the return of Line B, where higher return water temperatures are observed, to recover or reduce thermal energy before re-entering the central system. This would lower compressor load and improve cycle efficiency.
- **Ice bank outlet temperature management:** Optimization of the control strategy for the ice bank outlet so that the supply temperature is aligned with the lowest temperature requirement of the connected processes, preventing unnecessary overcooling of the system.
- **Falling film heat exchanger integration:** Implementing a falling film heat exchanger directly at the ice bank's outlet feeding Line B would enable precise temperature control for processes that require chilled water near 0°C. This approach reduces energy use while providing sufficient cooling.
- **Life-cycle cost analysis:** Incorporation of economic evaluation methods to compare proposed technical solutions not only from an energy perspective but also from a financial return on investment standpoint.
- **Integration with renewable energy:** Analysis of the potential integration of renewable energy sources, such as photovoltaic or thermal solar systems, to partially supply the refrigeration plant and reduce dependence on the electrical grid.

- **Expansion to other utilities:** Extension of the KPI/OPI methodology to other utility systems in the plant, such as compressed air, steam, or hot water, creating a global energy efficiency monitoring framework.

These future works will enable the facility to transition from an efficiency analysis perspective to a continuous improvement cycle, supported by data, advanced control systems, and integrated energy management. Implementing these measures is expected to further increase system efficiency, lower operational costs, and strengthen the sustainability of the industrial site.

Bibliography

[1] ASHRAE. Ashrae handbook—refrigeration.

[2] Kai Wang, Magnus Eisele, Yunho Hwang, and Reinhard Radermacher. Review of secondary loop refrigeration systems. 2009. Accessed on: 9 August 2025.

[3] Riccardo Accorsi, Emilio Ferrari, Beatrice Guidani, Riccardo Manzini, and Michele Ronzoni. An optimization framework for energy-driven food cold chain network design. 2025. Accessed on: 9 August 2025.

[4] Vaishnav Venkata Subhadu, Abdulaziz Al Nafjan, Adrianus Indrat Aria, and Maryam Farsi. Hybrid cooling solutions for sustainable refrigeration: Retrofit and renewable integration. 2025. Accessed on: 9 August 2025.

[5] Poul Alberg Østergaard, Sven Werner, Anders Dyrelund, Henrik Lund, Ahmad Arabkoohsar, Peter Sorknæs, Oddgeir Gudmundsson, Jan Eric Thorsen, and Brian Vad Mathiesen. The four generations of district cooling. 2022. Accessed on: 9 August 2025.

[6] EFAFLU. Bombas normalizadas, 2012.

[7] LOWARA. Horizontal centrifugal electric pumps equipped with ie2, ie3 motors, 2022.

[8] ISOTUBI. Informação técnica manual de instalação sistema numepress. `https://www.isotubi.com/wp-content/uploads/2021/03/manual_instalacio%CC%81n_PORT.pdf`. Acessed in: 8 of april of 2025.

[9] `file:///C:/Users/GA-PTV~1/AppData/Local/Temp/MicrosoftEdgeDownloads/5747a9e0-5ebf-4c90-9c67-5c0702124efe/PDF-Geral.pdf`. Acessed in: 8 of april of 2025.

[10] Comércio Central de Valado. K-flex st tubo. `https://www.isolamentos-ccv.com/produtos/k-flex-st-tubo/`. Acessed in: 8 of april of 2025.

[11] Lianying Zhanga, Zhenni Wanga, Xiaohu Yanga, Liwen Jina, Qunli Zhangb, and Wenju Hub. Thermo-economic analysis for directly-buried pipes insulation of district heating piping systems. 2017. Accessed on: 13 August 2025.

[12] Philip M. Gerhart, Andrew L. Gerhart, and John I. Hochstein. *Munson, Young and Okiishi's Fundamentals of Fluid Mechanics (nineth edition)*. John Wiley & Sons, Inc., 2021.

[13] metoblue. Dados históricos simulados de clima e tempo para vale de cambra. `https://www.meteoblue.com/pt/tempo/historyclimate/climatemodelled/vale-de-cambra_portugal_2733153`. Acessed in: 8 of april of 2025.

[14] Frank P. Incropera, David P. Dewitt, Theodore L. Bergman, and Adrienne S. Lavine. *Fundamentals of Heat and Mass Transfer (sixth edition)*. John Wiley & Sons, Inc., 2007.

Chapter A

Appendix

A.1 Diagram of circuit of chill compressors

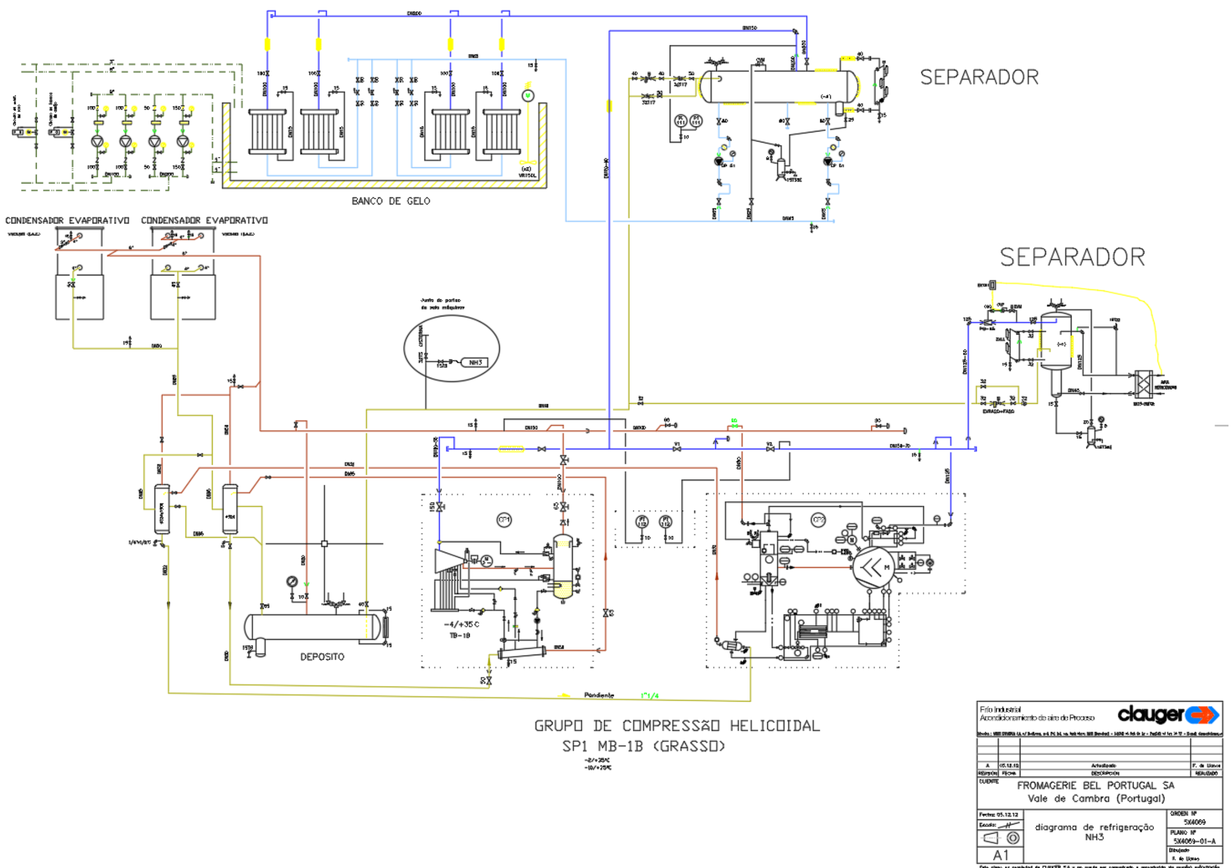

Figure A.1: Diagram of circuit of chill compressors

A.2 Catalogs of pumps

A.2.1 Line A

2900 rpm

TIPO TYPE	Ø (mm) DNA	DND	POTÊNCIA POWER HP	kW	CAUDAL I DELIVERY m³/h, l/min — l/min m³/h	83 5	133 8	267 16	333 20	417 25	500 30	583 35	667 40	833 50	1000 60	1167 70	1333 80	1583 95	1833 110	2167 130	2666 160	3000 180	3333 200	3667 220	4000 240	4333 260
					ALTURA MANOMÉTRICA TOTAL I TOTAL HEAD m																					
32-125/1,1/2	50	32	1,5	1,1		17	15	13	12	9	4,5	-														
32-125/1,5/2	50	32	2	1,5		20	19	17	15	12	9															
32-125/2,2/2	50	32	3	2,2		26	25	23	21	18	14,5	9,5														
32-125/3/2	50	32	4	3		27,5	27	25,5	23	20,5	16,5	12														
32-160/3/2	50	32	4	3		32	31	30	27,5	25	22															
32-160/4/2	50	32	5,5	4		38	37	36	34,5	32,5	28															
32-200/3/2	50	32	4	3		36	34,5	23,5					-	-	-	-	-	-	-	-	-	-	-	-	-	-
32-200/4/2	50	32	5,5	4		45	42,5	32	-																	
32-200/5,5/2	50	32	7,5	5,5		55	53	44		-		-														
32-200/7,5/2	50	32	10	7,5		65	63	54,5	37,5		-															
32-250/7,5/2	50	32	10	7,5		67	65	57	51																	
32-250/11/2	50	32	15	11		87	85	78	71	62																
32-250/15/2	50	32	20	15		108	105	97	91	83	70															
40-125/1,5/2	65	40	2	1,5		17	17	16	15	13,5	12	9	7,5	-												
40-125/2,2/2	65	40	3	2,2		22	22	21	19,5	19	17	15	13	7,5												
40-125/3/2	65	40	4	3		27,5	27	26,5	25,5	25	22	20	18	13	-											
40-160/3/2	65	40	4	3				26	25	24	22	20	13	11												
40-160/4/2	65	40	5,5	4				32	31	29,5	27	25,5	23	18												
40-160/5,5/2	65	40	7,5	5,5				39	37	36	35	34	32	26	17											
40-200/5,5/2	65	40	7,5	5,5				40	39,5	38	35	33	28	-		-	-	-	-	-	-	-	-	-	-	-
40-200/7,5/2	65	40	10	7,5				48	47,5	46	45	43	40	29	-											
40-200/11/2	65	40	15	11		-	-	65	64,5	64	63	61	58	55	32											
40-250/11/2	65	40	15	11				66	62	60	55	52	48	-												
40-250/15/2	65	40	20	15				80	78	75	72	68	63	54	-											
40-250/18,5/2	65	40	25	18,5				92	90	88	84	80	77	67												
40-250/22/2	65	40	30	22				105	102	100	96	92	89	79	62											
50-125/2,2/2	65	50	3	2,2				15	15	14,5	13	12,8	12,7	11,5	8	-										
50-125/3/2	65	50	4	3				18,5	18	18	17,5	17,2	17	15	12,5	9	-									
50-125/4/2	65	50	5,5	4				22,5	22	22	21,5	21,2	21	19,5	17	14,5	11	-								
50-125/5,5/2	65	50	7,5	5,5				26,5	26	26	25,5	25,3	25	24	22	19,5	16									
50-160/5,5/2	65	50	7,5	5,5					28	28	27	26,5	26	25,5	23,5	20,5	17		-							
50-160/7,5/2	65	50	10	7,5					35	35	34,5	34,3	34	33	30,5	27,5	25	17,5		-						
50-160/11/2	65	50	15	11					43	43	42,5	42	41,8	40	37	35	33	26,5								
50-200/11/2	65	50	15	11		-	-		40,5	40,2	40	40	39,5	37,5	36	33	30	25			-	-	-	-	-	-
50-200/15/2	65	50	20	15					50	49,8	49,7	49,6	48	47	46	43	40	35	27,5							
50-200/18,5/2	65	50	25	18,5				-	57	56,6	56,5	56,5	56	55	53	51	48	43	36							
50-200/22/2	65	50	30	22					65	64,8	64,7	64,7	64	62,5	61	58	56	52,5	45	34						
50-250/15/2	65	50	20	15					62	62	61,8	61,6	60	58	53	47	-									
50-250/18,5/2	65	50	25	18,5					72	72	71,8	71,6	70	67,5	58	56	51	-								
50-250/22/2	65	50	30	22					81	81	80,8	80,7	79,8	77	68	66	61,5		-	-						
50-250/30/2	65	50	40	30					99	99	98,8	98,6	98	94	86	85	80	76								

Figure A.2: Manometric height in function of delivery and bomb type in catalog EFAFLU [6]

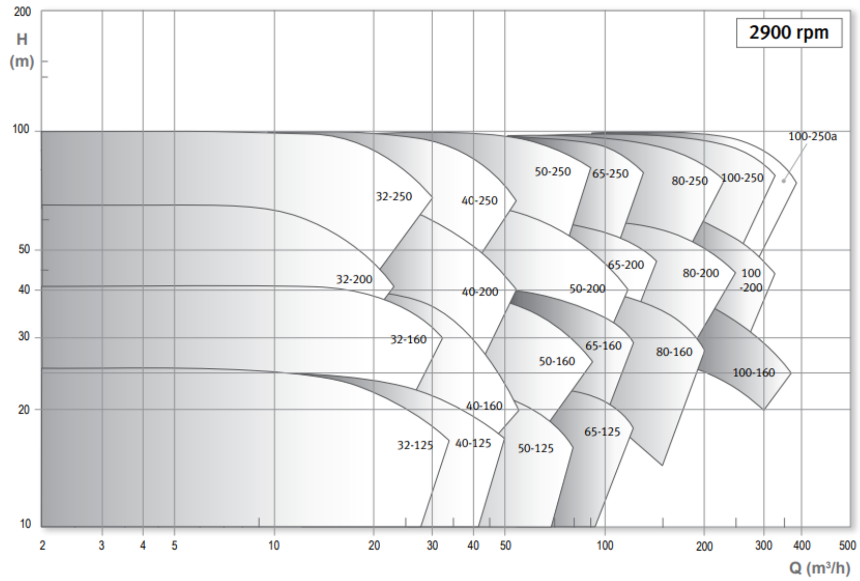

Figure A.3: Height graphic in catalog EFAFLU [6]

A.2.2 Line B

PUMP TYPE	P_N	Ø Impeller (mm)				Q = DELIVERY												
		STD	⊞	Ø	ηp %	l/s 0	11	22,5	33,8	45,1	56,3	67,6	78,9	90,2	101,4	112,7	124	135
						m^3/h 0	40	81	122	162	203	243	284	325	365	406	446	487
	kW	(1)		(2)	(3)	H = TOTAL HEAD METRES COLUMN OF WATER												
100-160/150	15	144	144	○	76,7	24,7	24,8	24,6	23,8	22,3	19,9	16,6	12,6					
100-160/185	18,5	156	156	○	79,7	29,1		28,7	28,2	26,9	24,6	21,3	17,1					
100-160/220	22	167	167	○	80,5	34,1		33,4	32,8	31,5	29,3	26,0	21,7	16,7				
100-160/300	30	187	187	●	83,8	44,1		42,7	41,9	40,6	38,7	35,9	32,1	27,1				
100-200/300	30	188	188	○	79,7	46,5		45,7	44,8	42,7	39,2	34,3	28,1	21,0				
100-200/370	37	202	202	○	82,0	53,9		53,4	52,8	51,2	48,2	43,8	38,0	31,0				
100-200/450	45	213	213	○	83,4	60,4		59,8	59,5	58,3	55,7	51,8	46,4	39,7	31,8			
100-200/550	55	227	227	●	84,6	69,2		68,9	68,2	66,9	64,7	61,3	56,6	50,6	43,0			
100-250/450	45	213	213	○	80,4	58,7		58,3	58,0	56,9	54,4	50,3	44,8	38,5	31,5			
100-250/550	55	227	227	○	83,1	67,8		67,7	67,4	66,2	64,0	60,5	55,7	49,6	42,4			
100-250/750	75	249	249	○	84,3	82,8		82,7	82,5	81,8	80,0	76,9	72,4	66,7	60,2	52,9		
100-250/900	90	259	259	●	85,0	90,1		90,1	89,8	88,8	87,0	84,0	79,8	74,4	67,6	59,6		
100-316/1100	110	270	270	○	78,6	104,7		104,3	103,5	101,9	99,3	95,6	90,5	83,7	74,6	62,4		
100-316/1320	132	286	286	○	79,9	116,6		116,2	115,7	114,2	111,8	108,5	104,2	98,6	91,4	81,5	67,3	
100-316/1600	160	302	302	●	80,8	131,3		130,9	130,8	129,9	128,0	124,8	120,4	115,0	108,8	101,5	91,8	77,0

Figure A.4: Manometric height in function of delivery and bomb type in catalog LOWARA [7]

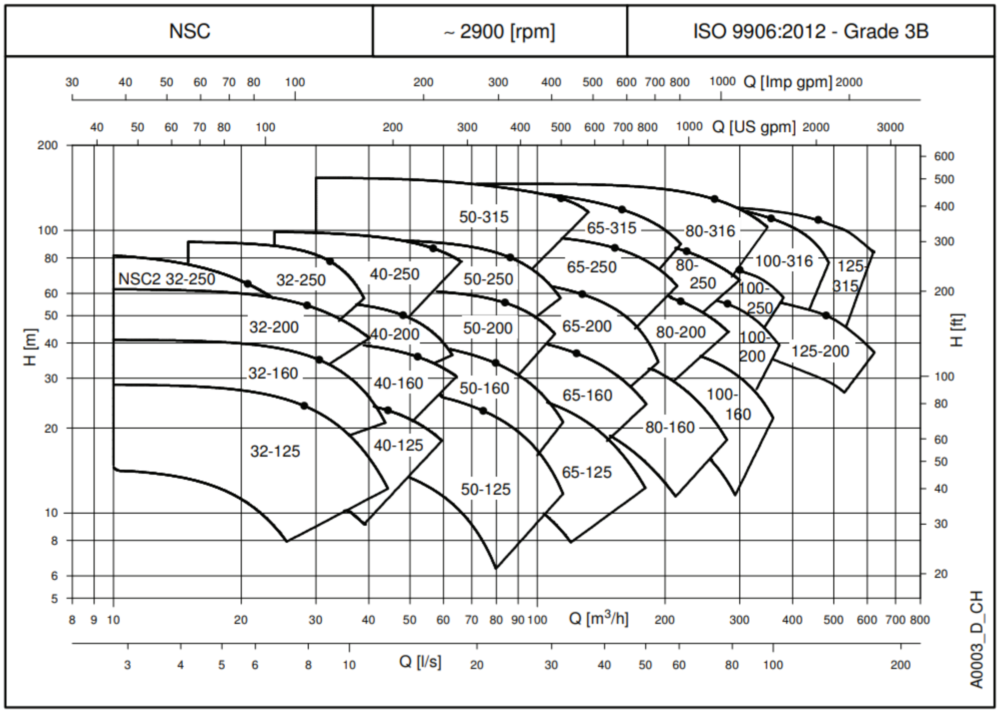

Figure A.5: Height graphic in catalog LOWARA [7]

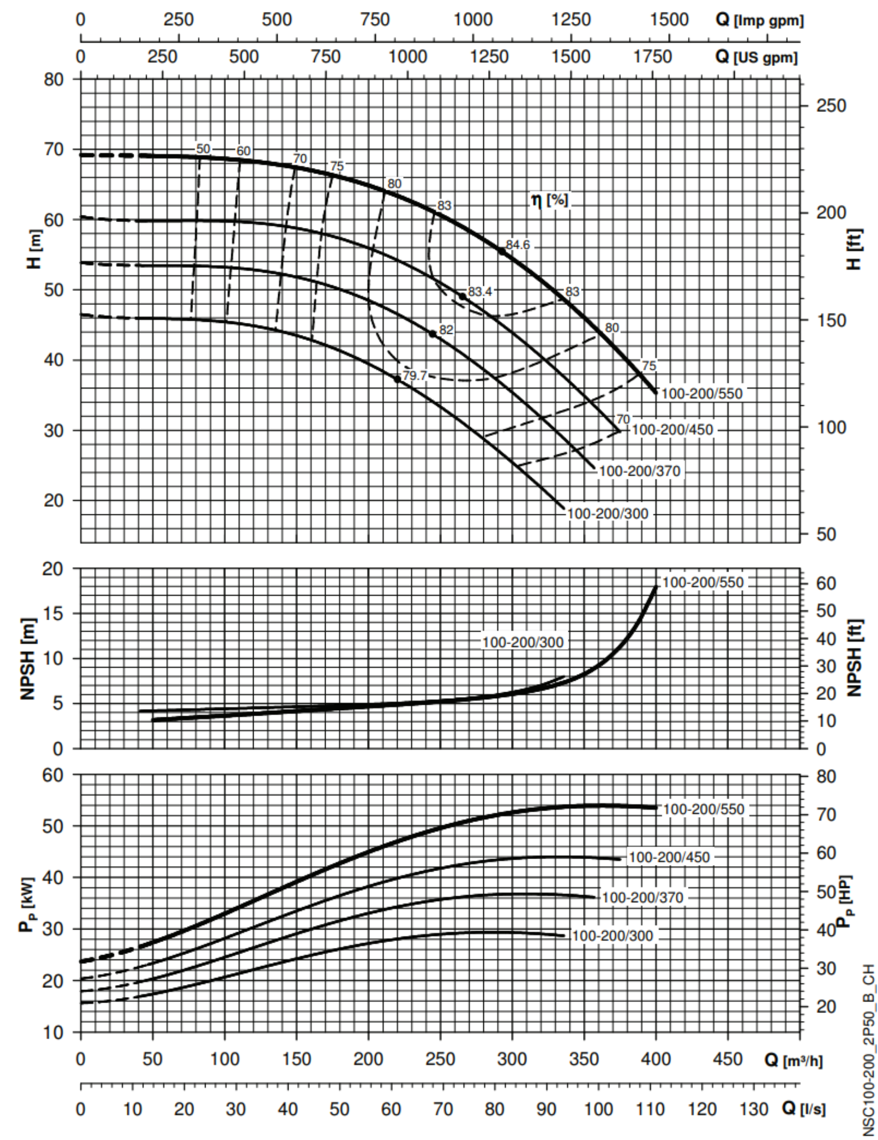

Figure A.6: NPSH, power and manometric height of pump in catalog LOWARA [7]

A.3 Physical properties of air and water

A.3.1 Water properties

Tab. A2 - Propriedades Físicas da Água

T (^oC)	P (atm)	ρ (kg/m^3)	c_p (KJ/KgK)	k (W/mK)	$\mu \times 10^6$ ($N.s/m^2$)	$\upsilon \times 10^6$ (m^2/s)	$\beta \times 10^3$ (K^{-1})	Pr	q_{lv} (KJ/Kg)	$\sigma \times 10^3$ (N/m)
0	1,00	999,8	4,218	0,552	1790,5	1,792	-0,070	13,67	2501	75,64
10	1,00	999,7	4,192	0,578	1306,3	1,304	0,088	9,47	2477	74,23
20	1,00	998,2	4,182	0,598	1001,6	1,004	0,207	7,01	2454	72,75
30	1,00	995,65	4,179	0,614	796,7	0,801	0,303	5,43	2430	71,20
40	1,00	992,2	4,179	0,628	651,7	0,658	0,385	4,34	2406	69,60
50	1,00	988,0	4,181	0,641	545,9	0,553	0,457	3,56	2382	67,94
60	1,00	983,2	4,184	0,651	465,5	0,474	0,523	2,99	2358	66,24
70	1,00	977,8	4,190	0,661	403,8	0,413	0,585	2,56	2333	64,47
80	1,00	971,8	4,197	0,669	354,8	0,365	0,643	2,23	2308	62,67
90	1,00	965,3	4,205	0,676	314,6	0,326	0,698	1,96	2283	60,82
100	1,03	958,4	4,216	0,682	277,3	0,295	0,752	1,75	2257	58,91
120	2,02	943,1	4,246	0,685	234,2	0,249	0,860	1,45	2203	54,96
140	3,68	928,1	4,287	0,684	198,9	0,215	0,975	1,25	2145	50,85
160	6,30	907,4	4,342	0,682	171,5	0,189	1,098	1,09	2083	46,58
180	10,23	886,8	4,409	0,678	150,4	0,170	1,233	0,98	2015	42,19
200	15,86	864,7	4,497	0,665	136,4	0,158	1,392	0,92	1941	37,69

Figure A.7: Physical properties of water at different temperatures

For water at Ti= 1ºC (interpolation between values of 0ºC and 10ºC)

- $\rho = 999.7\,\mathrm{kg/m^3}$
- $c_p = 4.2\,\mathrm{kJ/(kg \cdot K)}$
- $k = 0.56\,\mathrm{W/(m \cdot K)}$
- $\beta = 0.01 \times 10^{-3}\,\mathrm{K^{-1}}$
- $\nu = 1.6 \times 10^{-6}\,\mathrm{m^2/s}$
- $\mu = 1600 \times 10^{-6}\,\mathrm{N \cdot s/m^2}$
- $\mathrm{Pr} = 13$

A.3.2 Air properties

Tab. A1 - Propriedades Físicas do Ar								
T (ºC)	ρ (kg/m³)	c_p (KJ/KgK)	k (W/mK)	μ x 10^6 (N.s/m²)	υ x 10^6 (m²/s)	β x 10^3 (K^{-1})	D (m²/h)	Pr
-50	1,5340	1,005	0,0204	14,641	9,55	4,51	0,048	0,725
0	1,2930	1,005	0,0243	17,189	13,30	3,67	0,067	0,715
10	1,2488	1,005	0,0250	17,684	14,21	3,55	0,072	0,714
20	1,2045	1,005	0,0257	18,179	15,11	3,43	0,076	0,713
30	1,1656	1,005	0,0264	18,645	16,04	3,32	0,081	0,712
40	1,1267	1,005	0,0271	19,110	16,97	3,20	0,086	0,711
50	1,0931	1,005	0,0278	19,561	17,94	3,10	0,091	0,710
60	1,0595	1,009	0,0285	20,012	18,90	3,00	0,096	0,709
70	1,0297	1,009	0,0292	20,463	19,92	2,92	0,101	0,709
80	0,9998	1,009	0,0299	20,913	20,94	2,83	0,107	0,708
100	0,9458	1,009	0,0314	21,795	23,06	2,68	0,118	0,703
120	0,8968	1,013	0,0328	22,648	25,23	2,55	0,130	0,700
140	0,8535	1,013	0,0343	23,491	27,55	2,43	0,143	0,695
160	0,8170	1,017	0,0358	24,314	29,85	2,32	0,155	0,690
180	0,7785	1,022	0,0372	25,127	32,29	2,21	0,168	0,690
200	0,7457	1,026	0,0386	25,823	34,63	2,11	0,182	0,685

Figure A.8: Physical properties of air at different temperatures

For air in T room = 22ºC (Approximate values of 20ºC)

- $\rho = 1.2045\,\mathrm{kg/m^3}$
- $c_p = 1.005\,\mathrm{kJ/(kg \cdot K)}$
- $k = 0.0257\,\mathrm{W/(m \cdot K)}$
- $\beta = 3.43 \times 10^{-3}\,\mathrm{K^{-1}}$
- $\nu = 15.11 \times 10^{-6}\,\mathrm{m^2/s}$
- $\mu = 18.79 \times 10^{-6}\,\mathrm{N \cdot s/m^2}$
- $\mathrm{Pr} = 0.713$

A.4 Data for each section of the lines

This annex presents the fundamental data required for the calculation of pressure drops and heat gains along the chilled water distribution lines. The parameters provided include: D, the tube diameter with insulation; d_{ext}, the external diameter of the tube; d_{int}, the internal diameter of the tube; and l, the total pipe length. In addition, the annex details the flow rate, the Reynolds number (Re), the friction factor (f), and the fluid velocity (v). These parameters form the basis for the hydraulic and thermal analyses developed.

Section	D (mm)	d ext (mm)	d int (mm)	L total (m)	Caudal (m3/s)	Re	f	v (m/s)
1	200	63,5	60,3	1,7	0,004166667	52242,673	0,02128	1,45977
2	205	63,5	60,3	92,1845	0,002083333	26121,337	0,02461	0,72989
3	205	63,5	60,3	106,8505	0,002083333	26121,337	0,02461	0,72989
4	120	63,5	60,3	63,3935	0,001041667	13060,668	0,02907	0,36494
5	140	63,5	60,3	25,343	0,001041667	13060,668	0,02907	0,36494
6	110	38	35,6	0,6	0,000208333	4365,0129	0,03966	0,20941
7	80	38	35,6	11,3695	0,000260417	5456,2661	0,03711	0,26176
8	80	38	35,6	18,148	0,000260417	5456,2661	0,03711	0,26176
9	110	51	48,6	3,4915	0,000260417	4065,4531	0,04044	0,14045
10	95	51	48,6	1,936	0,000260417	4065,4531	0,04044	0,14045
11	115	38	35,6	44,921	0,001041667	21825,064	0,02599	1,04703
12	115	32	29,6	8,168	0,001041667	25917,264	0,02522	1,51452
13	200	63,5	60,3	42,8405	0,000347222	4353,5561	0,03955	0,12165
14	200	63,5	60,3	4,166	0,000173611	2176,7781	0,04955	0,06082
15	200	63,5	60,3	25,807	0,001041667	13060,668	0,02907	0,36494
16	110	38	35,6	0,959	0,000389984	8170,96	0,03313	0,39199
0	200	129	125	9,034	0,008333333	51432,71	0,02093	0,67941
total				460,912			0,02842	

Figure A.9: Data and properties of each section in the line A1

Section	D (mm)	d ext (mm)	d int (mm)	L total (m)	Caudal (m3/s)	Re	f	v (m/s)
1	205	63,5	60,3	77,3265	0,004166667	52242,673	0,02128	1,45977
2	205	63,5	60,3	110,681	0,002083333	26121,337	0,02461	0,72989
3	120	63,5	60,3	63,795	0,001041667	13060,668	0,02907	0,36494
4	140	63,5	60,3	25,343	0,001041667	13060,668	0,02907	0,36494
5	110	38	35,6	0,6	0,000208333	4365,0129	0,03966	0,20941
6	80	38	35,6	18,148	0,000260417	5456,2661	0,03711	0,26176
7	80	38	35,6	11,3695	0,000260417	5456,2661	0,03711	0,26176
8	110	51	48,6	3,4915	0,000260417	4065,4531	0,04044	0,14045
9	95	51	48,6	1,936	0,000260417	4065,4531	0,04044	0,14045
10	115	38	35,6	44,921	0,001041667	21825,064	0,02599	1,04703
11	32	32	29,6	9,4315	0,001041667	25917,264	0,02522	1,51452
12	200	63,5	60,3	42,8405	0,000347222	4353,5561	0,03955	0,12165
13	200	63,5	60,3	24,1075	0,000260417	3265,1671	0,04329	0,09124
14	200	63,5	60,3	3,26	0,001041667	13060,668	0,02907	0,36494
15	110	38	35,6	0,959	0	0	0	0
total				438,21			0,02861	

Figure A.10: Data and properties of each section in the line A2

Section	D (mm)	d ext (mm)	d int (mm)	L total (m)	Caudal (m3/s)	Re	f	v (m/s)
1	300	129	125	2,008	0,006944444	44232,13022	0,021321926	0,566171
2	300	129	125	5,341	0,013888889	88464,26044	0,018329799	1,132343
3	305	129	125	203,705	0,006944444	44232,13022	0,021321926	0,566171
4	300	129	125	32,8105	0,006944444	44232,13022	0,021321926	0,566171
5	250	129	125	3,1035	0,002314815	14744,04341	0,027849828	0,188724
6	160	63,5	60,3	6,678	0,002290765	30246,39001	0,023315122	0,802558
7	160	51	48,6	3,522	0,000763588	12509,30945	0,029102696	0,411829
8	160	51	48,6	3,522	0,000763588	12509,30945	0,029102696	0,411829
9	160	38	35,6	1,633	0,000763588	17077,31571	0,026855534	0,76752
10	120	63,5	60,3	3,87	0,002290765	30246,39001	0,023315122	0,802558
11	120	63,5	60,3	5,922	0,001145382	15123,195	0,027682391	0,401279
12	120	63,5	60,3	5,512	0,001145382	15123,195	0,027682391	0,401279
13	190	63,5	60,3	7,302	0,001736111	22922,95306	0,024926585	0,608238
14	190	63,5	60,3	5,393	0,000578704	7640,984352	0,03332182	0,202746
15	190	40	37	3,754	0,000578704	12452,73936	0,029149145	0,538497
16	190	40	37	0,439	0,000289352	6226,369682	0,035365961	0,269248
17	190	40	37	0,472	0,000289352	6226,369682	0,035365961	0,269248
18	120	63,5	60,3	11,805	0,001736111	22922,95306	0,024926585	0,608238
19	140	76,1	72,9	25,9165	0	0	0	0
20	130	76,1	72,9	50,282	0,002314815	25281,28156	0,024331018	0,55487
21	155	76,1	72,9	45,9755	0,000385802	4213,546927	0,039781116	0,092478
22	140	51	48,6	7,889	0,000385802	6320,32039	0,035203492	0,208076
23	130	63,5	60,3	9,8575	0,000385802	5093,989568	0,037532667	0,135164
24	145	63,5	60,3	34,514	0,001736111	22922,95306	0,024926585	0,608238
25	155	85	81	13,11	0,000385802	3792,192234	0,041118727	0,074908
26	100	51	48,6	25,8515	0,000385802	6320,32039	0,035203492	0,208076
27	190	101,6	97,6	13,885	0,000462963	3776,650463	0,041170532	0,061912
28	110	51	48,6	32,91	0,000231481	3792,192234	0,041125867	0,124846
29	130	76,1	72,9	13,3865	0,000578704	6320,32039	0,035195607	0,138718
30	100	38	35,6	26,294	0,000289352	6471,226916	0,034970691	0,290842
31	100	38	35,6	26,458	7,2338E-05	1617,806729	0,054960584	0,07271
32	330	101,6	97,6	13,6095	0,000289352	2360,406539	0,048067184	0,038695
33	85	85	83	8,5635	0,000578704	5551,221162	0,036570784	0,107011
0	300	129	125	7,6515	0,013888889	88464,26044	0,018329799	1,132343
total				662,946			0,028307074	

Figure A.11: Data and properties of each section in the line B1

Section	D (mm)	d ext (mm)	d int (mm)	L total (m)	Caudal (m3/s)	Re	f	v (m/s)
1	300	129	125	11,551	0,013888889	8846,426044	0,03196254	1,132343
2	300	129	125	202,013	0,006944444	4423,213022	0,039180876	0,566171
3	300	129	125	32,8105	0,006944444	4423,213022	0,039180876	0,566171
4	250	129	125	3,1035	0,002314815	1474,404341	0,056866665	0,188724
5	160	63,5	60,3	6,678	0,002290765	3024,639001	0,044234444	0,802558
6	63,5	63,5	60,3	3,87	0,002290765	3024,639001	0,044234444	0,802558
7	63,5	63,5	60,3	6,6315	0,001145382	1512,3195	0,05633684	0,401279
8	63,5	63,5	60,3	5,512	0,001145382	1512,3195	0,05633684	0,401279
9	190	63,5	60,3	7,953	0,002290765	3024,639001	0,044234444	0,802558
10	190	63,5	60,3	6,776	0,000578704	764,0984352	0,073858877	0,202746
11	40	40	37	6,2885	0,001157407	2490,547873	0,047207185	1,076994
12	120	63,5	60,3	11,805	0,001736111	2292,295306	0,048557266	0,608238
13	200	63,5	60,3	26,58	0	0	0	0
14	200	63,5	60,3	50,575	0,002314815	3056,393741	0,044083043	0,810983
15	155	85	81	44,137	0,000385802	379,2192234	0,101941607	0,074908
16	140	51	48,6	7,889	0,000385802	632,032039	0,080194811	0,208076
17	130	63,5	60,3	9,8575	0,000385802	509,3989568	0,088436414	0,135164
18	145	63,5	60,3	37,3925	0,001736111	2292,295306	0,048557266	0,608238
19	155	85	81	13,11	0,000385802	379,2192234	0,101941607	0,074908
20	100	51	48,6	25,8515	0,000385802	632,032039	0,080194811	0,208076
21	190	101,6	97,6	13,885	0,000462963	377,6650463	0,102150216	0,061912
22	110	51	48,6	33,844	0,000231481	379,2192234	0,101944396	0,124846
23	130	76,1	72,9	13,3865	0,000578704	632,032039	0,080192095	0,138718
24	330	101,6	99,2	10,761	0,000289352	232,2335466	0,132355637	0,037457
25	100	38	35,6	37,188	7,2338E-05	161,7806729	0,164431761	0,07271
26	330	101,6	97,6	27,075	0,000289352	236,0406539	0,131140017	0,038695
total				629,449			0,06848811	

Figure A.12: Data and properties of each section in the line B2

A.5 Pressure drop in different sections of each line

In this section, the frictional and local pressure losses of each segment are calculated and then subtracted from the initial line pressure to determine the resulting pressure distribution along the network.

Table A.1: Table of Pressure Drop in different sections of Line A1

Line A1	Frictional Losses	Local Losses	Total	P outlet (Pa)
1	639.00	5165.74	5804.74	
2	10018.68	2063.63	12082.31	
3	11612.59	1997.06	13609.66	
4	2034.62	1724.13	3758.75	
5	813.39	133.14	946.52	
6	14.65	78.90	93.55	
7	405.91	128.43	534.34	
8	647.92	94.18	742.09	
9	28.64	102.54	131.19	
10	15.88	9.86	25.74	
11	17971.34	9643.90	27615.24	
12	7980.65	3611.47	11592.11	
13	207.83	64.72	272.54	
14	6.33	1.39	7.72	
15	828.28	159.77	988.04	
16	68.54	38.40	106.94	
0	349.04	2722.46	3071.50	
Total	53643.29	27739.71	81383.01	223616.99

Table A.2: Table of Pressure Drop in different sections of A2

Line A2	Frictional Losses	Local Losses	Total	P outlet (Pa)
1	29065.85004	20237.75118	49303.60121	
2	12028.89586	2596.290447	14625.18630	
3	2047.507644	1724.203143	3771.710787	
4	813.3864132	133.1430998	946.5295130	
5	14.65005854	78.90788756	93.55794610	
6	647.9156166	94.18259149	742.0982081	
7	405.9112080	111.3066990	517.2179070	
8	28.64488978	102.5477643	131.1926541	
9	15.88328988	9.860361951	25.74365183	
10	17971.34064	9644.297369	27615.63801	
11	9215.166600	3152.998517	12368.16512	
12	207.8250361	45.49055911	253.3155953	
13	72.00203940	56.37778134	128.3798207	
14	104.6300638	133.1430998	237.7731636	
15	0	0	0	
Total	72639.60939	38120.50050	110760.1099	112856.8843

Table A.3: Table of Pressure Drop in different sections of B1

Line B1	Frictional Losses	Local Losses	Total	P outlet (Pa)
1	54.88017277	777.1003156	831.9804884	
2	501.9559578	3044.310515	3546.266472	
3	5567.413145	5223.395936	10790.80908	
4	896.7360103	600.8507595	1497.586770	
5	12.30997274	48.06806076	60.37803350	
6	831.3021934	1658.056640	2489.358833	
7	178.7969452	864.7169399	1043.513885	
8	178.7969452	830.8064717	1009.603417	
9	362.7345010	10305.92374	10668.65824	
10	481.7519449	4507.338438	4989.090383	
11	218.8199089	897.4432784	1116.263187	
12	203.6702699	897.4432784	1101.113548	
13	558.1789764	2579.647559	3137.826536	
14	61.23299179	0	61.23299179	
15	428.6712640	963.8904018	1392.561666	
16	15.20527498	0	15.20527498	
17	16.34826832	0	16.34826832	
18	902.3969894	277.3814580	1179.778447	
19	0	0	0	
20	2582.664940	3916.612113	6499.277053	
21	107.2497221	70.74866892	177.9983910	
22	123.6678313	16.23104848	139.8988798	
23	56.02992540	35.61440942	91.64433482	
24	2638.316789	5584.613354	8222.930143	
25	18.66584471	10.51771941	29.18356413	
26	405.2476791	178.5415333	583.7892124	
27	11.22215212	7.759766145	18.98191826	
28	216.9674026	56.48404871	273.4514513	
29	62.16282777	91.37479144	153.5376192	
30	1092.103509	281.1736177	1373.277127	
31	107.9422063	37.26078956	145.2029959	
32	5.016429054	4.041544867	9.057973922	
33	21.59772559	103.8908182	125.4885438	
0	719.1005450	7082.027618	7801.128163	
Total	19639.15726	50953.26564	70592.42290	379407.5771

Table A.4: Table of Pressure Drop in different sections of B2

Line B2	Frictional Losses	Local Losses	Total	P outlet (Pa)
1	1892.98075	4165.8986	6058.87935	
2	10145.6248	5207.37325	15352.998	
3	1647.8297	600.850759	2248.68046	
4	25.1357781	48.0680608	73.2038389	
5	1577.18199	482.929118	2060.11111	
6	914.000343	4507.33844	5421.33878	
7	498.676712	865.248004	1363.92472	
8	414.492353	865.248004	1279.74036	
9	1878.30613	3203.42928	5081.73595	
10	170.530649	0	170.530649	
11	4651.783	6000.7613	10652.545	
12	1757.87938	277.384158	2035.26384	
13	0	0	0	
14	12154.967	8366.64664	20521.6136	
15	155.797175	22.5780377	178.375213	
16	281.719731	16.2310485	297.950779	
17	445.020611	35.6144094	167.635021	
18	5568.10714	1839.96367	7408.07081	
19	46.2763887	10.5177194	56.7941801	
20	923.168668	176.377393	1099.54606	
21	27.843987	7.75976615	35.5997531	
22	593.059934	16.4840487	609.575042	
23	141.630609	52.901195	194.537264	
24	0.600782	2.62988496	3.2306674	
25	4591.18601	63.868815	4655.05482	
26	27.227485	9.50511478	36.7325997	
Total	46023.0301	36885.4226	82935.6802	296471.8969

A.6 Heat gain in different sections of each line

Table A.5: Table of Q gain in different sections of A1

Section A1	R1	R2	R3	R4	Q gain (W)
0	9.63E-06	3.701E-05	0.2147	0.094329	42.069
1	0.000106	0.00032	2.98509	0.501274	6.0227
2	1.96E-06	5.955E-06	0.0562	0.000019	321.788
3	1.69E-06	5.137E-06	0.048515	0.007781	372.983
4	2.84E-06	8.659E-06	0.044048	0.022404	314.261
5	7.11E-06	2.166E-05	0.137987	0.048036	112.871
6	0.000509	0.00115	7.8356	2.58232	2.015
7	2.69E-05	6.091E-05	0.289618	0.187379	44.017
8	1.68E-05	3.816E-05	0.18144	0.11739	70.261
9	6.407E-05	0.000146	0.97377	0.443671	14.812
10	0.000016	2.643E-05	1.4212	0.9266	8.9427
11	6.798E-06	1.54E-05	0.109036	0.03299	147.834
12	4.497E-05	0.0001013	0.69272	0.18144	24.018
13	4.21E-06	1.28E-05	0.118455	0.01989	151.774
14	4.33E-05	0.000131	1.21811	0.20455	14.759
15	6.06E-06	2.127E-05	0.196639	0.03302	91.429
16	0.000318	0.00072	4.9046	1.615633	3.221
total					1714.073

Table A.6: Table of Q gain in different sections of A2

Section A2	R1	R2	R3	R4	Q gain (W)
1	1.852E-05	7.0987E-06	0.0670388	0.0107516	214.608
2	1.294E-05	4.9594E-06	0.0468362	0.0075115	307.179
3	2.245E-05	8.6044E-06	0.0441823	0.0222631	251.421
4	5.561E-05	2.1659E-05	0.137987	0.0480361	89.736
5	0.0040428	0.00115429	7.8356972	2.5823201	16.65
6	0.0001337	3.8163E-05	0.1814425	0.1173911	55.851
7	0.0004563	2.963E-05	0.2896186	0.1877398	34.9904
8	0.0005348	0.005106	0.9737716	0.4436121	17.755
9	0.0009178	0.0002431	1.412114	0.9266699	7.109
10	5.4E-05	1.5418E-05	0.1070561	0.0495149	12.46
11	0.0003093	8.775E-05	0	0.5647071	29.552
12	3.343E-05	1.2813E-05	0.1184546	0.0198916	120.571
13	0.000542	2.2769E-05	0.155685	0.0593203	56.11
14	0.0004393	0.00016838	1.5566419	0.2614005	9.182
15	0	0	0	0	0
total					1319.111

Table A.7: Table of Q gain in different sections of B1

section B1	R1	R2	R3	R4	Q gain (W)
0	2.863E-05	4.37E-05	0.4878	0.0592	38.374
1	0.000109105	0.000167	1.85909	0.225917	10.071
2	4.10191E-05	6.26E-05	0.8943	0.084936	26.786
3	1.07549E-05	1.64E-06	0.1868	0.00219	622.668
4	6.7722E-06	1.02E-05	0.11378	0.013826	164.551
5	7.05922E-05	0.000108	0.943	0.175405	18.773
6	6.8E-05	8.22E-05	0.61211	0.12737	28.392
7	0.000159996	0.00145	1.43591	0.241504	12.513
8	0.0001599	0.00145	1.43591	0.241504	12.513
9	0.000471	0.000424	3.89391	0.241504	4.7557
10	0.000117352	0.000142	0.72743	0.05853	20.573
11	7.6889E-05	9.27E-05	0.47573	0.1915	31.482
12	8.239E-05	9.96E-06	0.5107	0.20575	29.302
13	6.21955E-05	7.52E-05	0.6639	0.098093	27.554
14	8.42114E-05	0.000102	0.9889	0.132816	20.351
15	0.00019798	0.00022	1.83591	0.1908	10.359
16	0.001685979	0.001885	15.6993	1.63106	1.211
17	0.001568103	0.001753	14.617	1.51732	1.303
18	3.84711E-05	4.65E-05	0.23847	0.09607	62.755
19	0	0	0	0	0
20	7.4709E-06	9.07E-06	0.04711	0.02082	309.086
21	8.1708E-06	9.2E-06	0.068	0.01909	148.476
22	7.14266E-05	6.49E-05	0.56619	0.123221	30.454
23	4.6077E-05	5.57E-05	0.3215	0.10642	49.087
24	1.31558E-05	1.12E-05	0.10704	0.074062	97.713
25	2.5788E-05	3.9E-05	0.2027	0.066973	77.854
26	2.1797E-05	1.98E-05	0.11521	0.052644	125.078
27	1.7122E-05	1.35E-05	0.19941	0.051556	83.648
28	2.39256E-05	2.18E-05	0.20903	0.074302	92.24
29	2.80623E-05	3.41E-05	0.17694	0.070203	82.287
30	2.925E-05	3.4E-05	0.1627	0.051576	97.864
31	2.90744E-05	2.62E-05	0.17513	0.051734	98.476
32	2.0617E-05	1.34E-05	0.38283	0.03032	50.819
33	3.85291E-05	2.95E-05	0	0.18966	112.222
total					2598.667

Table A.8: Table of Q gain in different sections of B2

section B2	R1	R2	R3	R4	Q gain (W)
1	8.47851E-05	2.895E-05	0.323181	0.0392729	46.887
2	4.84797E-06	1.655E-06	0.018479	0.002245	434.123
3	2.98488E-05	1.019E-05	0.113776	0.0138261	133.184
4	0.000315564	0.00010077	0.943004	0.1754049	15.194
5	0.000340008	8.22E-05	0.612106	0.12737	22.977
6	0.000524591	0.00011418	0	0.5537947	30.66
7	0.000036814	8.277E-05	0	0.328126	52.538
8	0.000039376	0.0001237	0	0.3182584	26.431
9	0.000255271	6.902E-05	0.609553	0.0900635	24.287
10	0.000040936	8.101E-05	0.715433	0.1007503	19.646
11	0.000526139	0.0001136	0	0.5410363	31.383
12	0.00017	4.65E-05	0.238472	0.0996097	50.782
13	0	0	0	0	0.0
14	4.01417E-05	1.085E-05	0.10039	0.0315445	149.322
15	3.42422E-05	1.159E-05	0.60207	0.0198929	24.551
16	0.000139842	4.56E-05	0.566185	0.12123	24.641
17	0.000025955	5.569E-05	0.321502	0.1061997	39.723
18	5.42934E-05	1.486E-05	0.005512	0.025104	73.264
19	0.000115228	9.36E-05	0.202696	0.0669729	83.041
20	9.73477E-05	9.18E-05	0.040127	0.1129935	62.313
21	9.03344E-05	0.0	0.119411	0.0158683	67.696
22	7.44271E-05	1.5E-05	0.14089	0.1073774	65.643
23	0.000012544	3.31E-05	0.482763	0.0385099	54.059
24	0.000012665	2.358E-05	0.448727	0.0338258	51.294
25	2.9469E-05	1.862E-05	0	0.0521338	32.541
26	4.63266E-05	1.575E-05	0.192457	0.0152318	81.829
total					1896.126

A.7 Frigorific capacity and inlet and return temperatures by the hour

Table A.9: Schedule Water Temperature and refrigeration capacity necessary Data

Schedule	T water inlet (°C)	T water outlet (°C)	Frigorific Capacity (kW)
1	2.5	26.5	1 819
2	4.5	26.5	1 667
3	3.5	28.5	1 895
4	4.5	28	1 781
5	4	28	1 819
6	4	28	1 819
7	5	28	1 743
8	1	28	2 046
9	1	28	2 046
10	1	28	2 046
11	1	29	2 122
12	3	26	1 895
13	3	29	1 971
14	4.5	24	1 478
15	4	27	1 743
16	3.5	26.5	1 705
17	3.5	27	1 781
18	5.5	28.5	1 743
19	4.5	28.5	1 819
20	3.5	28.5	1 895
21	4	28.5	1 857
22	3.5	28.5	1 895
23	3.5	28.5	1 857
24	3	27	1 819